PERFORMANCE ANALYSIS AND OPTIMIZATION OF RELAY-ASSISTED FREE SPACE OPTICAL COMMUNICATION SYSTEMS

A Thesis

by

Mohammadreza Amini Kashani

Submitted to the
Graduate School of Sciences and Engineering
In Partial Fulfillment of the Requirements for
the Degree of

Master of Science

in the
Department of Electrical and Electronics Engineering

Özyeğin University
July 2012

PERFORMANCE ANALYSIS AND OPTIMIZATION OF RELAY-ASSISTED FREE SPACE OPTICAL COMMUNICATION SYSTEMS

Approved by:

Professor Murat Uysal, Advisor
Department of Electrical and Electronics Engineering
Özyeğin University

Professor Ali Özer Ercan
Department of Electrical and Electronics Engineering
Özyeğin University

Professor Ali Emre Pusane
Department of Electrical and Electronics Engineering
Boğaziçi University

Date Approved: 01 August 2012

To My dear parents

ABSTRACT

Free-space optical (FSO) communication has received an increasing attention in recent years with its ability to achieve ultra-high data rates (at the order of multiple gigabits per second) over unlicensed optical spectrum. A major degrading factor, particularly in long links, is the atmospheric turbulence induced fading. Smartly exploiting the fact that fading variance is distance-dependent in the FSO channel, relay-assisted transmission takes advantage of the resulting shorter hops and yields significant performance improvements. In this thesis, we make several contributions to the performance analysis and design of relay-assisted FSO systems. In the first part, we investigate how to determine optimal relay locations in serial and parallel FSO relaying as to minimize the outage probability and quantify performance improvements obtained through optimal relay placement. In the second part, we investigate the combined use of serial and parallel relaying for FSO mesh networks. We derive the outage probability expressions of FSO mesh networks and demonstrate performance improvements with respect to both stand-alone serial and parallel relaying schemes. We also present a diversity gain analysis and quantify the achievable diversity orders in terms of the number of relays and turbulence channel parameters. Finally, we investigate the use of all-optical relaying removing the need for optical-electrical and electrical-optical conversions. Building on all-optical relay assumption, we investigate the outage performance of a dual-hop FSO link taking into account practical limitations such as amplifier noise and filtering effects.

ÖZETÇE

Kablosuz optik (KAO) iletişim, lisansız optik spektrumda ultra-yüksek veri hızına ulaşabilme (saniyede birkaç gigabit mertebesinde) kabiliyetiyle, son yıllarda giderek daha fazla artan bir ilgi çekmektedir. Ancak, atmosferik türbülansın sebep olduğu sönümleme, özelikle uzun linklerde, bu sistemlerin başarımını önemli derecede etkileyen olumsuz bir faktördür. Sönümleme varyansının, KAO kanalında uzaklığa bağlı olduğu gerçeğinden yararlanarak ortaya atılan röle yardımlı iletim teknikleri önemli başarım iyileştirmeleri sağlamaktadır. Bu tez çalışmasında, röle yardımlı KAO sistemlerinin başarım analizi ve tasarımı konularında literatüre çeşitli katkılar sağlanmıştır. Tezin ilk bölümünde, seri ve paralel KAO röle sistemlerinde servis dışı kalma olasılığını en küçükleyen optimal röle konuşlandırması belirlenmiş ve optimal röle konuşlandırması durumunda sağlanan başarım artışı nicemlenmiştir. Tezin ikinci bölümde, KAO ağlarında seri ve paralel röle sistemlerinin birlikte kullanımı incelenmiştir. KAO ağlar için servis dışı kalma olasılık ifadeleri çıkarılmış ve paralel ve seri rölelemenin tek başlarına olan kullanımlarına göre başarım artışları ortaya konmuştur. Ayrıca çeşitleme kazanç analizi sunulmuş ve elde edilebilir çeşitleme derecesi röle sayısı ve türbülans kanal parametreleri cinsinden formülleştirilmiştir. Son olarak, optik-elektrik ve elektrik-optik çevirici ihtiyacı ortadan kaldıran tüm-optik röle kullanımı incelenmiştir. Tüm-optik röle varsayımı altında, yükselteç gürültüsü ve filtreleme etkisi gibi pratik sınırlamalar da göz önüne alınarak, çift-atlamalı bir KAO linki için servis dışı kalma olasılığı çıkarımı yapılmıştır.

ACKNOWLEDGEMENTS

Foremost, I would like to express my utmost gratitude to my supervisor, Professor Murat Uysal, for his excellent guidance, motivation and immense knowledge. This thesis would have not been possible without his consistence support throughout the course of my M.Sc. studies. I consider it an honor to work with him.

I would like to sincerely acknowledge the members of my dissertation committee, Professors Ali Özer Ercan and Ali Emre Pusane for taking the time to carefully read my thesis.

I am indebted to all my friends especially Sepideh, Shahab, Hatef, Hamza, Ekrem for their kindness and moral support during my study. Thanks for the friendship and memories.

Last, but by no means least, I owe my deepest gratitude to my dear parents for their endless love and sincere encouragement and inspiration throughout my life. They have lifted me uphill this phase of life.

TABLE OF CONTENTS

LIST OF TABLES

LIST OF FIGURES

CHAPTER I

INTRODUCTION

Wireless optical communication (WOC) [1, 2] refers to unguided optical transmission via the use of either lasers or light emitting diodes (LEDs). WOC can be classified into two main categories as indoor and outdoor systems. Indoor WOC is characterized by short transmission range and free from major outdoor environmental degradations such as rain, snow, building sway, and atmospheric turbulence. Outdoor WOC is commonly referred to as free-space optical (FSO) communication and is categorized as satellite-based and terrestrial-based links, the latter of which will be the focus of this thesis.

Terrestrial FSO systems offer significant advantages such as higher bandwidth capacity, an unregulated spectrum, and robustness to the electromagnetic interference as well as transparency to the traffic types and protocols. These systems have initially attracted attention as an efficient solution for the "last mile" problem to bridge the gap between the end user and the fiber optic infrastructure already in place. They are also appealing for a wide range of applications such as metropolitan area network (MAN) extension, local area network (LAN)-to-LAN connectivity, fiber back-up, backhaul for wireless cellular networks, disaster recovery, high definition TV and medical image/video transmission, wireless video surveillance/monitoring, and quantum key distribution among others.

Despite the major advantages of FSO technology and variety of its application areas, its widespread use has been hampered by its rather disappointing link reliability particularly in long ranges due to atmospheric turbulence-induced fading. Atmospheric turbulence occurs as a result of the variations in the refractive index due to

inhomogeneties in temperature and pressure changes [3]. This results in rapid fluctuations at the received signal, i.e., signal fading, severely impairing the link performance. Although FSO links are built taking into account a certain dynamic margin, the practical limitations on power budgets do not allow very high margins leaving the link vulnerable to deep fades. Powerful temporal and spatial diversity techniques need to be deployed for FSO links particularly with transmission range of 1 km or longer.

As a form of temporal diversity, channel coding can be employed in FSO communications to combat fading [4–6]. However, optical links with their transmission rates of order of gigabits exhibit high temporal correlation. For fixed-rate error-correction codes, this requires large-size interleavers to achieve the promised coding gains. Deployment of rateless codes (e.g., punctured codes, fountain codes) whose rate can be modified to accommodate a time-varying channel quality has been further investigated for FSO links [7, 8]. Based on the temporal characteristics of turbulence-induced fading, maximum likelihood sequence detection (MLSD) is proposed in [9] as another solution for fading mitigation. MLSD requires complicated multidimensional integrations and suffers from excessive computational complexity. Some sub-optimal temporal-domain fading mitigation techniques are further explored in [9–11].

Spatial diversity techniques [12], i.e., deployment of multiple receive and/or receive apertures, provide an attractive approach for fading compensation with their inherent redundancy. Besides their role as a fading-mitigation tool, multiple-aperture designs significantly reduce the potential for temporary blockage of the laser beam by obstructions (e.g., birds, cranes) and allow a greater total transmission power (due to regulatory power constraints on individual lasers). Information theoretic bounds for multiple-input multiple-output (MIMO) FSO links have been first studied in [13], where ergodic capacity and outage capacity are derived for intensity-modulation/direct-detection (IM/DD) FSO links operating in log-normal modeled atmospheric turbulence. Under the assumption of shot-noise-limited regime with

Poisson statistics, it is demonstrated in [13] that ergodic capacity scales as the number of transmit apertures times the number of receive apertures for high signal-to-background noise ratio. Since then, MIMO FSO communication has been extensively investigated in the literature [13–22] under the assumption of different turbulence channel models (e.g., log-normal, gamma-gamma, negative exponential) and noise regimes (e.g., Gaussian, Poisson, Webb).

Another method to exploit spatial diversity in FSO links is relay-assisted cooperative communication. Cooperative diversity has been originally introduced in the context of wireless radio-frequency (RF) communication (see e.g., [23] and the references therein) and depends on the notion of network nodes helping each other in relaying information to realize spatial diversity advantages in a distributed manner. The concept of cooperative communication has been applied to FSO communications in [24–30]. While initial studies [24–27] have demonstrated the usefulness of relay-assisted transmission as a method to broaden the coverage area, the study in [28] highlighted its use as a fading-mitigation tool. In [28], Safari and Uysal have considered two relay-assisted schemes, namely *serial relaying* (i.e., multi-hop transmission) and *parallel relaying* (i.e., cooperative diversity) and derived the outage performance for each scheme assuming both amplify-and-forward (AF) and decode-and-forward (DF) relaying. They have shown that relay-assisted FSO systems exploit the fact that fading variance is distance-dependent in atmospheric turbulence channels and yield significant performance improvements by taking advantage of the resulting shorter hops.

Building upon the framework of [28], this thesis makes several contributions to the performance analysis and design of relay-assisted FSO systems. The key contributions, which have been either published or submitted by the author [31–35] during the course of this research, are summarized as follows:

- For DF FSO relaying schemes, we formulate optimization problems based on

the minimization of end-to-end outage probability to determine optimal relay locations. Our results demonstrate that for serial relaying the minimum outage probability is achieved when the relay nodes are placed equidistant along the direct line from the source to the destination. On the other hand, in parallel relaying, the optimal relay locations turn out to be a function of the signal-to-noise ratio (SNR), the number of relays, and end-to-end link distance.

- We present a diversity gain analysis for serial and parallel DF relaying schemes and quantify their diversity advantages in terms of the number of relays and channel parameters over log-normal turbulence channels. Our asymptotical analysis reveals that diversity gains of $(N+1)^{11/6}$ and $2^{11/6}N$ are available, respectively, for serial and parallel relaying configurations where N denotes the number of relays.

- Since FSO is a line-of-sight technology, a practical FSO mesh network would be likely to deploy a combination of serial and parallel relaying. In this part, we extend the results of [28] to this general and more practical scenario and derive the outage performance of a multi-hop parallel DF FSO network. Our outage probability analysis demonstrates substantial performance improvements with respect to both stand-alone serial and parallel relaying schemes. Then, based on the outage performance of *multi-hop parallel* FSO network, we present a diversity gain analysis and quantify the achievable diversity orders in terms of the number of relays and turbulence channel parameters. Our analysis yields that a diversity order of $(K+1)^{11/6}(N/K)$ is achievable (with K denoting the number of relaying groups) for a multi-hop parallel relaying scheme.

- The current literature on amplify-and-forward (AF) relaying in FSO systems [26, 28, 36, 37] builds on the assumption that relays employ optical-electrical (OE) and electrical-to-optical (EO) convertors. The actual advantage of AF

relaying over the DF counterpart emerges if its implementation avoids the requirement for high-speed (at the order of GHz) electronics and electro-optics. This becomes possible with *all-optical* AF relaying where the signals are processed in optical domain and the relay requires only low-speed electronic circuits to control and adjust the gain of amplifiers [38]. Therefore, EO/OE domain conversions are eliminated, allowing efficient implementation. In the last part, we investigate the performance of a dual-hop FSO link with an all-optical AF relay. We employ photon counting methodology and derive closed form expressions for the end-to-end signal-to-noise ratio and the outage probability. In our derivations, we consider either full or partial channel state information (CSI) at the relay and take into account practical limitations such as amplifier noise and filtering effects. Our results indicate significant performance improvements over direct transmission and furthermore demonstrate that semi-blind relaying (which depends only on statistical CSI) provides nearly identical performance to its full-CSI counterpart.

The rest of the thesis is organized as follows: In Chapter 2, we briefly describe the channel model under consideration. In Chapter 3, we investigate the optimal relay placement problem for cooperative FSO systems with DF relaying and present the optimized outage performance. Furthermore, we derive the achievable diversity gains for serial and parallel relaying. In Chapter 4, we propose multi-hop parallel FSO scheme and present the outage performance and diversity gains assuming DF relaying. In Chapter 5, we investigate the performance of a dual-hop FSO optical link with an all-optical AF relay. Finally, we conclude in Chapter 6.

CHAPTER II

ATMOSPHERIC TURBULENCE CHANNEL MODEL

When a laser beam propagates through the atmosphere, the light field is attenuated owing to absorption and scattering. It is well known that gaseous molecules of the atmosphere along with bad weather conditions such as rain, snow, fog, etc. cause absorption and scattering. The path loss of the optical link with length d is defined as [39]

$$l(d) = e^{-\sigma d} \frac{A_{TX} A_{RX}}{(\lambda d)^2}, \tag{1}$$

where A_{TX}, A_{RX}, λ are respectively the transmitter aperture area, the receiver aperture area, the wavelength, and σ denotes the attenuation coefficient which is made up of scattering and absorption components.

In addition to the path loss, the optical links may experience fading due to the turbulent atmosphere. In this respect, the spatial and temporal variations of the air thermal inhomogeneities lead to variations of the refractive index along the transmission path. These random refractive index variations (i.e., atmospheric turbulence) can cause power losses at the receiver and eventually amplitude fluctuations (scintillation) and phase variations (aberration) of an optical wave propagating through the atmosphere [3].

In the classical *Rytov method* [39], the atmosphere turbulent medium is assumed to consist of several thin slabs. Base on this assumption, each slab modulates the optical field from the previous slab's perturbation by some incremental amount of $\exp(\chi_i + j\varphi_i)$ where χ_i and φ_i denote, respectively, the first-order log-amplitude and phase of the field. Therefore, the received electric field can be written in terms of the

transmitted field, U_0 as

$$U = U_0 \exp(\chi + j\varphi) = U_0 \prod_i \exp(\chi_i + j\varphi_i) = U_0 \exp\left(\sum_i \chi_i + j \sum_i \varphi_i\right). \quad (2)$$

According to the central limit theorem the fading log-amplitude, $\chi = \sum_i \chi_i$, and phase, $\varphi = \sum_i \varphi_i$, have normal distributions. Consequently, the turbulence-induced fading amplitude, $|\alpha| = \exp(\chi)$, is a *log-normal* random variable with the probability distribution function (pdf) given by

$$p(|\alpha|) = \frac{1}{|\alpha| \sqrt{2\pi\sigma_\chi^2}} \exp\left(-\frac{(\ln(|\alpha|) - \mu_\chi)^2}{2\sigma_\chi^2}\right), \quad (3)$$

where μ_χ and σ_χ^2 are respectively the mean and the variance of the random variable χ. Based on the Rytov theory and assuming spherical wave propagation through a horizontal atmospheric path, the log-amplitude variance is given by [39]

$$\sigma_\chi^2(d) = \min\left\{0.124 k^{7/6} C_n^2 d^{11/6}, 0.5\right\}, \quad (4)$$

where k is the wave number and C_n^2 is the refractive index structure constant and the minimum is taken to consider the case of saturated scintillation. The validity of log-normal model under weak turbulence conditions has been confirmed by numerous experiments [39].

In this thesis, we consider an aggregated channel model where both path loss and turbulence-induced fading are taken into account. The channel coefficient of an optical link is given by

$$A = |\alpha|^2 L(d), \quad (5)$$

where $L(d) = \ell(d)/\ell(d_{S,D})$ denotes the *normalized path loss* with respect to the distance of the direct link between the source and the destination, i.e., $d_{S,D}$. In (5) we normalize the fading amplitude such that $E[|\alpha|^2] = 1$ implying $\mu_x = -\sigma_x^2$. This ensures that the fading does not attenuate or amplify the average power [14].

CHAPTER III

OPTIMAL RELAY PLACEMENT AND DIVERSITY ANALYSIS OF RELAY-ASSISTED FSO COMMUNICATION SYSTEMS

Relay-assisted FSO transmission exploits the fact that atmospheric turbulence fading variance is distance dependent and yields significant performance gains by taking advantage of the resulting shorter hops [28]. In this chapter, building on the framework of [28] we investigate how to determine optimal relay locations in serial and parallel DF FSO relaying as to minimize the outage probability and quantify performance improvements obtained through optimal relay placement. We further present a diversity gain analysis for serial and parallel FSO relaying schemes and quantify their diversity advantages in terms of the number of relays and channel parameters.

3.1 System Model

We consider an intensity-modulation direct-detection (IM/DD) FSO system assuming the deployment of binary pulse position modulation (BPPM). Under the assumption of BPPM deployment, information is conveyed with the presence or absence of light where the optical transmitter is "on" during one half of the BPPM bit interval (i.e., "signal slot") and is "off" during the other half (i.e., "non-signal slot"). In serial DF relaying (Fig. 1), the source node transmits a BPPM signal to a relay node. The relay decodes the signal after direct detection, modulates it with BPPM, and retransmits it to the next relay. This continues until the source's data arrives at the destination node. In parallel DF relaying (Fig. 2), the source node is equipped with a multi-laser transmitter with each of the transmitter pointing out in the direction of

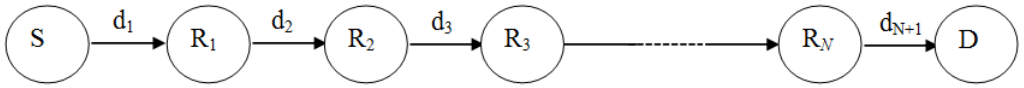

Figure 1: FSO serial relaying configuration.

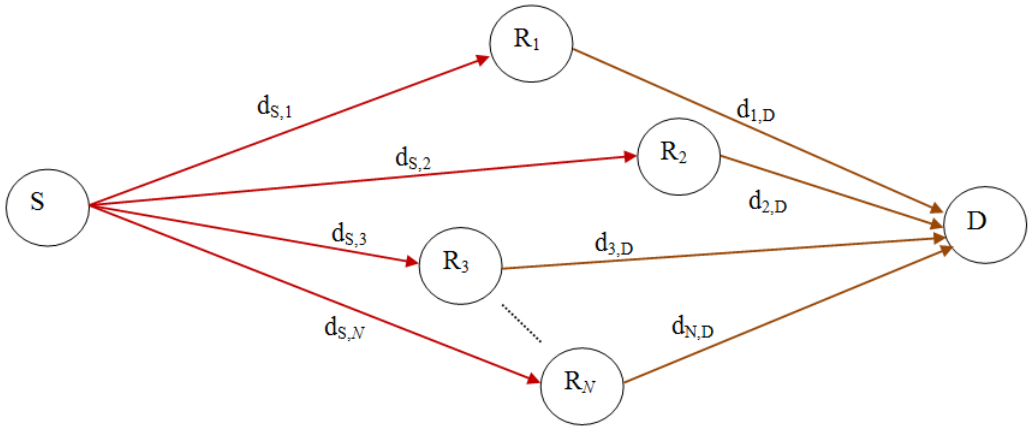

Figure 2: FSO parallel relaying configuration.

a corresponding relay node. It transmits the same signal to N relay nodes and each relay decodes and retransmits the signal to the destination only if their received SNR exceeds a given decoding threshold.

3.2 Outage Probability for FSO Relaying Schemes

Let R_0 denote a targeted transmission rate and let $\gamma_{th} = C^{-1}(R_0)$ be the corresponding SNR threshold in terms of instantaneous channel capacity corresponding to a fading channel realization. The outage probability is given by $P_{out}(R_0) = \Pr(\gamma < \gamma_{th})$ [40]. If SNR exceeds γ_{th}, no outage happens and the receiver can decode the signal with arbitrarily low error probability.

In the following, we provide the outage probability expressions for serial and parallel DF relaying for the convenience of the reader (see [28] for details of derivation). In serial DF relaying, an outage occurs when any of the intermediate single-input single-output (SISO) links fails. Therefore, the outage probability of the end-to-end

link can be expressed as

$$P_{out} = \Pr\left(\bigcup_{i=1}^{N+1} \{\gamma_i < \gamma_{th}\}\right) = 1 - \prod_{i=1}^{N+1} (1 - \Pr(\gamma_i < \gamma_{th})), \tag{6}$$

where γ_i $(1 \leq i \leq N+1)$ denotes the SNR of the i^{th} intermediate SISO link. Assuming a signal-independent additive white Gaussian noise with zero mean and variance of $\sigma_n^2 = N_0/2$, γ_i is given by $\gamma_i = R^2 T_b^2 P^2 A_i^2 / N_0$. Here, A_i is the channel gain of the i^{th} intermediate SISO link with length d_i, T_b is the duration of the signal/non-signal slots, R is responsitivity of the photodetector, and P is the average transmitted optical power per transmit aperture which is related to the total transmit power by $P = P_t/(N+1)$ for serial DF relaying. Starting from (6), the end-to-end outage probability of the serial DF relaying scheme can be obtained as [28]

$$P_{out} = 1 - \prod_{i=1}^{N+1} \left(1 - Q\left(\frac{\ln\left(L(d_i) P_M/(N+1)\right) + 2\mu_\chi(d_i)}{2\sigma_\chi(d_i)}\right)\right), \tag{7}$$

where P_M denotes power margin and is defined as $P_M = \sqrt{P_t^2 R^2 T_b^2 / N_0 \gamma_{th}}$.

In parallel relaying, an outage occurs if none of the relay nodes decode the signal successfully or multiple-input single-output (MISO) link between the correctfully-decoding relays and the destination fails. The *decoded set* is defined as the set of relays having successfully decoded the signal and consists of 2^N possibilities. Let $W(i)$ denote the i^{th} possible set, and $\bar{d}_{W(i)}$ denote the set of all distances between the destination and the relays in the decoded set, i.e., $d_{j,D} \in \bar{d}_{W(i)}, \forall j \in W(i)$. The corresponding outage probability is given by [28]

$$P_{out} = \sum_{i=1}^{2^N} P_{out-p}(W(i)) = \sum_{i=1}^{2^N} \left[\prod_{\mathrm{j}\in \mathrm{W(i)}} \left(1 - Q\left(\frac{\ln\left(\frac{L\left(d_{S,j}\right)P_M}{2N}\right) + 2\mu_\chi\left(d_{S,j}\right)}{2\sigma_\chi\left(d_{S,j}\right)}\right)\right)\right.$$
$$\left.\prod_{\mathrm{j}\notin W(\mathrm{i})} Q\left(\frac{\ln\left(\frac{L\left(d_{S,j}\right)P_M}{2N}\right) + 2\mu_\chi\left(d_{S,j}\right)}{2\sigma_\chi\left(d_{S,j}\right)}\right)\right] Q\left(\frac{\ln\left(\frac{P_M e^{\mu_\xi}}{2N}\right)}{\sigma_\xi\left(\bar{d}_{W(i)}\right)}\right), \tag{8}$$

where $\mu_\xi(\bar{d}_{W(i)})$ and $\sigma_\xi^2(\bar{d}_{W(i)})$ are given by

$$\mu_\xi(\bar{d}_{\mathrm{W}(i)}) = \ln \sum_{i\in \mathrm{W}(i)} L(d_{i,D}) - \sigma_\xi^2(\bar{d}_{\mathrm{W}(i)})/2, \tag{9}$$

$$\sigma_\xi^2(\bar{d}_{\mathrm{W}(i)}) = \ln \left(1 + \sum_{i\in \mathrm{W}(i)} L^2(d_{i,D})(e^{4\sigma_\chi^2} - 1) / \left(\sum_{i\in \mathrm{W}(i)} L(d_{i,D}) \right)^2 \right). \tag{10}$$

3.3 Optimization of Relay Location

In this part, we aim to optimize the end-to-end outage probability for serial and parallel FSO relaying schemes with respect to relay(s) location(s).

3.3.1 Serial DF Relaying

The end-to-end outage probability for serial DF relaying is given by (7). We need to minimize (7) with respect to the length of the intermediate SISO links (d_i) in Fig. 1. Let $d_1, d_2, \ldots$ and d_{N+1} denote these lengths to be optimized and define the following functions

$$h\left(d_1, d_2, \ldots, d_{N+1}\right) = \prod_{\mathrm{i}=1}^{N+1} \Phi\left(f\left(d_i\right)\right), \tag{11}$$

$$g\left(d_1, d_2, \ldots, d_{N+1}\right) = \sum_{i=1}^{N+1} d_i, \tag{12}$$

where $\Phi(x) = 1 - Q(x)$ is the cumulative distribution function of the normal Gaussian distribution [41], and $f(d_i)$ is given by

$$f\left(d_i\right) = \frac{\ln\left(L\left(d_i\right) P_M / (\ N+1)\right) + 2\mu_\chi\left(d_i\right)}{2\sigma_\chi\left(d_i\right)}. \tag{13}$$

It can be readily verified that the optimum place for each relay is on the direct path from the source to the destination (see Section A.1, Theorem I). Now, the optimization problem can be stated as

$$\begin{aligned} \max_{d_1, d_2, \ldots, d_{N+1}} \quad & h\left(d_1, d_2, \ldots, d_{N+1}\right) \\ \text{s.t.} \quad & g\left(d_1, d_2, \ldots, d_{N+1}\right) = d_{S,D}. \end{aligned} \tag{14}$$

Since $f(d_i)$ is a monotonically decreasing function, $h(.)$ is found to be a concave function with respect to optimization parameters. By applying Lagrange multiplier method, we obtain $N+1$ equations where the i^{th} equation ($i = 1, 2, \ldots, N+1$) can be expressed as

$$f'(d_i) \exp\left(-\frac{f(d_i)^2}{2}\right) \prod_{\substack{j=1 \\ j \neq i}}^{N+1} \Phi(f(d_j)) = 2\Lambda\sqrt{2\pi} \tag{15}$$

with Λ denoting the Lagrange multiplier. Since Λ is a constant, all the $N+1$ equations are equal to each other. Therefore, for the i^{th} and k^{th} equations ($1 \leq i, k \leq N+1$), we can write

$$f'(d_i) \exp\left(-\frac{f(d_i)^2}{2}\right) \Phi(f(d_k)) = f'(d_k) \exp\left(-\frac{f(d_k)^2}{2}\right) \Phi(f(d_i)). \tag{16}$$

Noting that $f'(d_i) \exp\left(-f(d_i)^2/2\right) / \Phi(f(d_i))$ is a monotonically decreasing function, the solution of (16) is found as

$$d_i = d_k. \tag{17}$$

Hence, the outage probability is minimized when the consecutive nodes are placed equidistant along the path from the source to the destination.

3.3.2 Parallel DF Relaying

Let $d_{S,j}$ and $d_{j,D}$, $j = 1, 2, ...N$, respectively denote the distance of source-to-relay and relay-to-destination links. The end-to-end outage probability for parallel DF relaying is given by (8) which will be minimized with respect to $d_{S,j}$, $d_{j,D}$, $j = 1, 2, ...N$. It can be shown that, for performance optimization in parallel relaying, all the relays should be located along the direct path from the source to the destination (see Section A.2, Theorem II). However, a closed-form analytical solution for optimized locations is not

readily available. Defining the following functions

$$z(d_{S,1}, d_{S,2}, \ldots, d_{S,N}, d_{1,D}, \ldots, d_{N,D}) \tag{18}$$
$$\stackrel{def}{=} \sum_{i=1}^{2^N} \left[\prod_{\mathrm{j}\in \mathrm{W(i)}} \left(1 - Q\left(u(d_{S,j})\right)\right) \prod_{\mathrm{j}\notin \mathrm{W(i)}} Q\left(u(d_{S,j})\right) \right] \times Q\left(v(\bar{d}_{W(i)})\right),$$

$$u(d_{S,j}) \stackrel{def}{=} \left(\ln\left(\frac{L\left(d_{S,j}\right) P_M}{2N} \right) + 2\mu_\chi\left(d_{S,j}\right) \right) / 2\sigma_\chi\left(d_{S,j}\right), \tag{19}$$

$$v(\bar{d}_{W(i)}) \stackrel{def}{=} \ln\left(\frac{P_M e^{\mu_\xi}}{2N} \right) / \sigma_\xi\left(\bar{d}_{W(i)}\right), \tag{20}$$

we can state the optimization problem as

$$\min_{d_{S,j}, d_{j,D}, j=1,2,..,N} \; z\left(d_{S,1}, d_{S,2}, \ldots, d_{S,N}, d_{1,D}, \ldots, d_{N,D}\right)$$
$$\text{s.t. } d_{S,j} + d_{j,D} = d_{S,D} \qquad j = 1, 2, ..., N. \tag{21}$$

This non-convex optimization problem can be solved by numerical methods. Here, we use the genetic algorithm [42] which is an adaptive heuristic search algorithm premised on the evolutionary ideas of natural selection and genetic. This algorithm creates a population of solutions and applies genetic operators such as mutation and crossover to evolve the solutions in order to find the best one. Genetic algorithms are frequently used in the literature on wireless communication for system optimization [43, 44].

Our numerical optimization through genetic algorithm shows that the optimum solution of (21) occurs if all of the relays (that should be located along the direct path from the source to the destination) are placed at exactly the same point. It should be noted that, in practice, due to the size of FSO transceivers, relay terminals cannot be obviously placed at the same physical location. However, as demonstrated later in our simulation results (see Section 3.4), placement of relay terminals (separated from each other by a distance more than the spatial coherence length) on the perpendicular line crossing the optimum location results in near-optimum performance.

Table 1 provides the optimized distances from the source, i.e. relay locations, for some given values of power margin (P_M), link range ($d_{S,D}$), number of relays (N),

wavelengths (λ), refractive index structure constant (C_n^2) and atmospheric attenuation (σ). It is observed from our results that the optimum position slightly decreases by increasing the wavelength while it slightly increases by increasing the refractive index structure constant. It is also observed that the optimum position is somewhere close to the source, and becomes closer as the number of relays increases or for the low values of power margin.

Based on the numerical optimization results (see Table 1), a heuristic expression can be further developed through an interpolation on logarithmic functions. This expression for optimum relay location is given by

$$d_{opt}(P_M, d_{S,D}, N) = 0.5 d_{S,D} + \frac{\eta}{\mathrm{P}_M} \ln(\varpi \mathrm{P}_M^{\kappa} + \Delta), \quad N \geq 2, \tag{22}$$

where η, ϖ, κ and Δ are defined, respectively, as

$$\begin{aligned}
\eta &= d_{S,D}\left(7 \times 10^{-6} d_{S,D} - 0.14 \ln(N) - 0.5\right), \\
\varpi &= -2.7 \times 10^{-5} d_{S,D} + 0.1 \ln(N) + 0.11, \\
\kappa &= -6.5 \times 10^{-6} d_{S,D} + 1.19, \\
\Delta &= 4.5 \times 10^{-5} d_{S,D} + 0.024 N + 0.9.
\end{aligned}$$

Table 1: Normalized optimal relay locations for parallel relaying

$\lambda = 1550nm$, $\sigma \approx 0.1$ and $C_n^2 = 10^{-14}\mathrm{m}^{2/3}$. The unit of $d_{S,D}$ is kilometers. N denotes the number of relays. Since optimization has yielded the same location for all relays, only one numerical value is provided regardless of the relay number.

	$N=2$		$N=3$		$N=4$		$N=5$	
P_M	$d_{S,D}=3$	$d_{S,D}=5$	$d_{S,D}=3$	$d_{S,D}=5$	$d_{S,D}=3$	$d_{S,D}=5$	$d_{S,D}=3$	$d_{S,D}=5$
$[dB]$	Optimal Relay Locations							
0	0.4037	0.3997	0.3575	0.3389	0.3191	0.3001	0.2812	0.2731
5	0.4334	0.4472	0.4012	0.4160	0.3778	0.3906	0.3582	0.3698
10	0.4466	0.4617	0.4239	0.4432	0.4104	0.4260	0.3945	0.4121
15	0.4660	0.4705	0.4489	0.4588	0.4393	0.4488	0.4360	0.4443
20	0.4781	0.4871	0.4705	0.4791	0.4686	0.4710	0.4635	0.4680

3.4 Outage Performance Results

In this section, we present the optimized outage performance for serial and parallel relaying schemes under consideration. We consider an FSO system with $\lambda = 1550$ nm operating in clear weather conditions with a visibility of 10 km. The end-to-end link range is $d_{S,D} = 5$ km, the atmospheric attenuation is 0.43 dB/km (i.e., $\sigma \approx 0.1$), and refractive index structure constant is $C_n^2 = 10^{-14}\text{m}^{2/3}$. The log-amplitude variance is therefore calculated as $\sigma_\chi^2 = 0.38$ below the saturation regime.

In Fig. 3, we present the outage performance for serial DF relaying assuming $N = 3$ relays. Some arbitrary chosen relay locations along with optimized relay locations are considered. Specifically, we have the following configurations

- **Scenario 0 (Optimized)**: $d_1 = d_2 = d_3 = d_4 = d_{S,D}/4$
- **Scenario 1**: $d_1 = d_4 = d_{S,D}/8, d_2 = \ d_3 = 3d_{S,D}/8$
- **Scenario 2**: $d_1 = d_2 = d_3 = d_{S,D}/5, d_4 = 2d_{S,D}/5$
- **Scenario 3**: $d_1 = d_2 = d_3 = d_{S,D}/6, d_4 = d_{S,D}/2$

It is observed from Fig. 3 that relay location optimization substantially improves the performance. At an outage probability of 10^{-6}, we achieve performance improvements of 7.2 dB, 8.2 dB and 13.4 dB respectively with respect to non-optimized scenarios 1, 2 and 3.

In Fig. 4, we present the optimized outage performance for parallel DF relaying assuming $N = 2, 3, 4, 5$ relays along with the equi-distant relay cases. The optimized relay locations are already given in Table 1. To reflect the performance in practical settings, we have also included the performance when the relay terminals are placed on the perpendicular line crossing the optimum location and separated from each other by a distance of 50 m. These two cases are labeled as "optimum" and "near-optimum". At a target outage probability of 10^{-6}, we observe performance improvements of 1.5

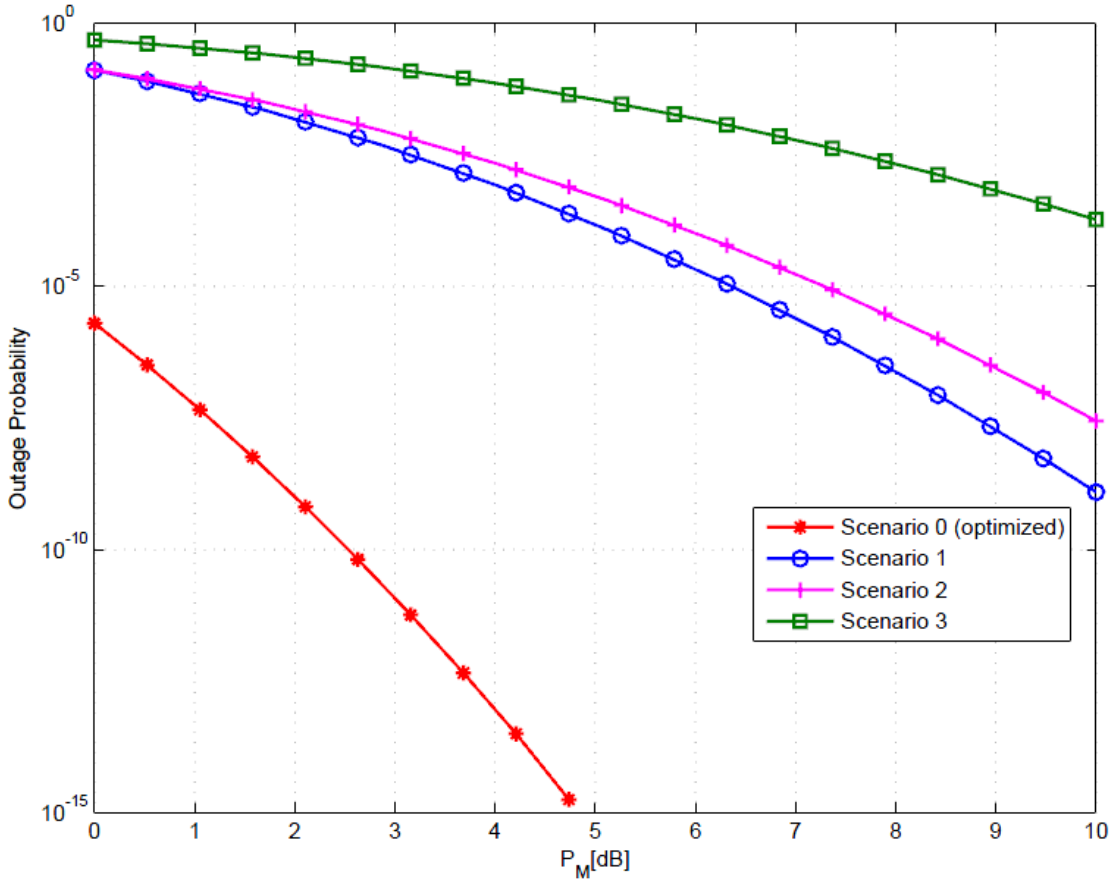

Figure 3: Outage probability of serial FSO relaying scheme for different scenarios.

dB, 1.7 dB, 2.8 dB, 4 dB respectively for $N = 2, 3, 4$ and 5 with respect to equi-distant located relays. Furthermore, it is observed that separation of the relay terminals results in a negligible performance degradation, i.e., within the line of thickness of outage probability plots. It is also demonstrated in Fig. 4 that the performance improvements of parallel relaying are less than those observed in serial relaying. This is as a result of the nature of parallel relaying in which there are only two hops that can be optimized regardless of relay numbers.

3.5 Diversity Gain Analysis

Diversity order is conventionally defined as the negative asymptotic slope of the error rate performance (e.g., bit error rate or outage probability) versus SNR on a log-log

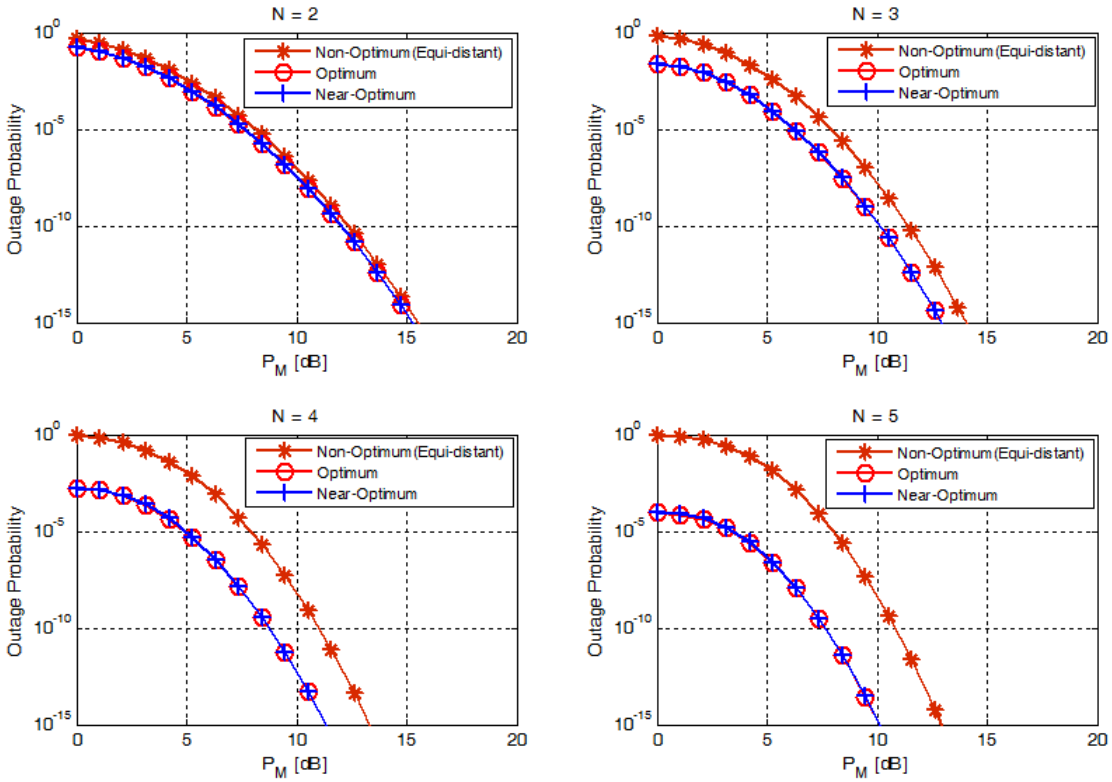

Figure 4: Outage probability of parallel FSO relaying scheme for different number of relays and scenarios.

scale [40]. As discussed in [45], the conventional definition of diversity order yields infinity and does not provide a meaningful measure for diversity order over log-normal fading channels. To overcome this problem, so-called "relative diversity order (RDO)" has been introduced in [45] which is given as

$$\mathrm{RDO}(P_M) = \frac{\partial \ln P_{out} / \partial \ln P_M}{\partial \ln P_{out,\mathrm{SISO}} / \partial \ln P_M}, \tag{23}$$

where $P_{out,SISO}$ is the outage probability of direct (SISO) transmission. The asymptotic relative diversity order (ARDO) can be further defined as

$$ARDO = \lim_{P_M \to \infty} RDO(P_M). \tag{24}$$

3.5.1 Serial Relaying

Calculation of RDO: Inserting (7) in (23), the RDO of FSO serial relaying scheme is obtained as

$$\mathrm{RDO}\left(P_M\right) = \frac{\partial \ln \left(1 - \prod_{\mathrm{i}=1}^{N+1} \left(1 - Q\left(\frac{\ln(L(d_i)P_M/N+1)+2\mu_\chi(d_i)}{2\sigma_\chi(d_i)}\right)\right)\right) / \partial \ln P_M}{\partial \ln \left(Q\left(\left(\ln\left(P_M\right) + 2\mu_\chi\left(d_{S,D}\right)\right)/2\sigma_\chi\left(d_{S,D}\right)\right)\right) / \partial \ln P_M}. \tag{25}$$

Expanding the product in the numerator and neglecting the higher order terms, (25) can be well approximated as

$$\mathrm{RDO}\left(P_M\right) \approx \frac{\partial \ln \left(\sum_{i=1}^{N+1} Q\left(\frac{\ln(L(d_i)P_M/N+1)+2\mu_\chi(d_i)}{2\sigma_\chi(d_i)}\right)\right) / \partial \ln P_M}{\partial \ln \left(Q\left(\left(\ln\left(P_M\right) + 2\mu_\chi\left(d_{S,D}\right)\right)/2\sigma_\chi\left(d_{S,D}\right)\right)\right) / \partial \ln P_M}, \tag{26}$$

which can be further rewritten as

$$\mathrm{RDO}\left(P_M\right) \approx \frac{\sum_{i=1}^{N+1} P_{out-s}\left(i\right) \frac{\partial ln P_{out-s}(i)}{\partial \ln P_M}}{\frac{\partial \ln\left(Q\left(\left(\ln(P_M)+2\mu_\chi\left(d_{S,D}\right)\right)/2\sigma_\chi\left(d_{S,D}\right)\right)\right)}{\partial \ln P_M} \sum_{i=1}^{N+1} P_{out-s}\left(i\right)}, \tag{27}$$

where $P_{out-s}\left(i\right) = Q\left(\left(\ln\left(P_M\right) + \psi(i)\right)/\left(2\sigma_\chi\left(d_i\right)\right)\right)$ and $\psi\left(i\right) = \ln\left(L\left(d_i\right)/N + 1\right) + 2\mu_\chi\left(d_i\right)$. Note that Q function can be bounded as [41]

$$\frac{1}{\sqrt{2\pi}} \frac{x}{1+x^2} \exp(-x^2/2) \; < Q(x) < \frac{1}{\sqrt{2\pi}x} \exp(-x^2/2). \tag{28}$$

Applying these bounds, we obtain an (approximate) upper and lower bound on (27) as

$$RDO\left(P_M\right) \overset{\sim}{\leq} \frac{\sum_{i=1}^{N+1}\left(\frac{\ln(P_M)+\ \psi(i)}{4\sigma_\chi^2(d_i)}+\frac{2\sigma_\chi(d_i)}{\ln(P_M)+\ \psi(i)}\right)\tilde{P}_{out-s}(i)}{\rho\sum_{i=1}^{N+1}\hat{P}_{out-s}}, \tag{29}$$

$$RDO\overset{\sim}{\geq}$$

$$\frac{\sum_{i=1}^{N+1}\left(\left(\frac{(\ln(P_M)+\psi(i))^2}{4\sigma_\chi^4(d_i)}-1\right)/\left(\frac{\ln(P_M)+\psi(i)}{2\sigma_\chi(d_i)}\left(1+\frac{(\ln(P_M)+\ \psi(i))^2}{4\sigma_\chi^4(d_i)}\right)\right)+\frac{\ln(P_M)+\psi(i)}{4\sigma_\chi^4(d_i)}\right)\hat{P}_{out-s}(i)}{\left(\frac{2\sigma_\chi(D)}{\ln(P_M)+2\mu_x(D)}+\frac{\ln(P_M)+2\mu_x(D)}{4\sigma_\chi^2(D)}\right)\sum_{i=1}^{N+1}\tilde{P}_{out-s}(i)}, \tag{30}$$

where

$$\tilde{P}_{out-s}=\frac{2\sigma_\chi\left(d_i\right)}{\ln(P_M)+\ \psi(i)}\exp\left(-\frac{\left(\ln\left(P_M\right)+\ \psi(i)\right)^2}{8\sigma_\chi^2\left(d_i\right)}\right) \tag{31}$$

$$\hat{P}_{out-s}=\left(\frac{\ln\left(P_M\right)+\ \psi(i)}{2\sigma_\chi\left(d_i\right)}/\left(1+\frac{\left(\ln\left(P_M\right)+\ \psi(i)\right)^2}{4\sigma_\chi^4\left(d_i\right)}\right)\right)\exp\left(-\frac{\left(\ln\left(P_M\right)+\ \psi(i)\right)^2}{8\sigma_\chi^2\left(d_i\right)}\right), \tag{32}$$

$$\rho=\left(\frac{2\sigma_\chi\left(d_{S,D}\right)\left(\left(\ln\left(P_M\right)+\ 2\mu_x\left(d_{S,D}\right)\right)^2-4\sigma_\chi^4\left(d_{S,D}\right)\right)}{\left(\ln\left(P_M\right)+\ 2\mu_x\left(d_{S,D}\right)\ \right)\left(4\sigma_\chi^4\left(d_{S,D}\right)+\left(\ln\left(P_M\right)+\ 2\mu_x\left(d_{S,D}\right)\right)^2\right)}\right.$$
$$\left.+\ \frac{\ln\left(P_M\right)+\ 2\mu_x\left(d_{S,D}\right)}{4\sigma_\chi^2\left(d_{S,D}\right)}\right). \tag{33}$$

Calculation of ARDO and maximum achievable ARDO: Taking the limits of (29) and (30) and employing the squeeze theorem [46], ARDO is obtained as

$$ARDO=\lim_{P_M\to\infty}\frac{\sigma_\chi^2\left(d_{S,D}\right)\sum_{i=1}^{N+1}\frac{1}{\sigma_\chi(d_i)}\exp\left(-\frac{(\ln(P_M))^2}{8\sigma_\chi^2(d_i)}\right)}{\sum_{i=1}^{N+1}\sigma_\chi\left(d_i\right)\exp\left(-\frac{(\ln(P_M))^2}{8\sigma_\chi^2(d_i)}\right)}=\frac{\sigma_\chi^2\left(d_{S,D}\right)}{\underset{d_i}{Max}\ \left(\sigma_\chi^2\left(d_i\right)\right)}, \tag{34}$$

which simplifies as

$$ARDO=\left(d_{S,D}/d_{max}\right)^{11/6}. \tag{35}$$

As expected from the earlier optimization results, maximum ARDO is achieved when the consecutive nodes are equi-distant along the direct link between the source and

the destination. Replacing $d_{max} = d_{S,D}/(N+1)$ in (35), we have

$$ARDO_{\max} = (N+1)^{11/6}. \tag{36}$$

3.5.2 Parallel Relaying

Calculation of RDO: Inserting (8) in (23), the RDO of FSO parallel relaying scheme is obtained as

$$\mathrm{RDO}(P_M) = \frac{\partial \ln \left(\sum_{i=1}^{2^N} P_{out-p}(W(i)) \right) / \partial \ln P_M}{\partial \ln \left(Q \left(\left(\ln \left(P_M \right) + 2\mu_\chi \left(d_{S,D} \right) \right) / 2\sigma_\chi \left(d_{S,D} \right) \right) \right) / \partial \ln P_M}. \tag{37}$$

The numerator of (37) can be rearranged as

$$I = \frac{\sum_{i=1}^{2^N} \frac{\partial P_{out-p}(W(i))}{\partial \ln P_M}}{\sum_{i=1}^{2^N} P_{out-p}(W(i))} = \frac{\sum_{i=1}^{2^N} P_{out-p}(W(i)) \frac{\partial \ln P_{out-p}(W(i))}{\partial \ln P_M}}{\sum_{i=1}^{2^N} P_{out-p}(W(i))}. \tag{38}$$

Furthermore, we can calculate $\partial ln P_{out-p}\left(W(i)\right) / \partial \ln P_M$ as

$$\begin{aligned} \frac{\partial ln P_{out-p}\left(W(i)\right)}{\partial \ln P_M} = & \frac{\partial}{\partial \ln P_M} \left(\sum_{\mathrm{j} \in \mathrm{W(i)}} \ln \left(1 - Q \left(\frac{\ln \left(P_M \right) + \ \upsilon(j)}{2\sigma_\chi \left(d_{S,j} \right)} \right) \right) \right. \\ & \left. + \sum_{\mathrm{j} \notin \mathrm{W(i)}} \ln \left(Q \left(\frac{\ln \left(P_M \right) + \ \upsilon(j)}{2\sigma_\chi \left(d_{S,j} \right)} \right) \right) + \ln \left(Q \left(\frac{\ln \left(P_M \right) + \tilde{\upsilon}(W(i))}{\sigma_\xi \left(\overline{d_{W(i)}} \right)} \right) \right) \right), \end{aligned} \tag{39}$$

where $\upsilon(j) = \ \ln \left(L \left(d_{S,j} \right) / 2N \right) + 2\mu_\chi \left(d_{S,j} \right)$ and $\tilde{\upsilon}(W(i)) = \mu_\xi \left(\bar{d}_{W(i)} \right) - \ln(2N)$. By combining (37), (38) and (39) and using the bounds on Q functions given by (28), upper and lower bounds on RDO are obtained as

$$\mathrm{RDO}\left(P_M\right) \leq \ \frac{\sum_{i=1}^{2^N} \tilde{P}_{out-p}\left(W(i)\right) \hat{\kappa}(i)}{\rho \sum_{i=1}^{2^N} \hat{P}_{out-p}\left(W(i)\right)}, \tag{40}$$

$$\mathrm{RDO}\left(P_M\right) \geq \ \frac{\sum_{i=1}^{2^N} \tilde{\kappa}(i) \hat{P}_{out-p}\left(W(i)\right)}{\left(\frac{2\sigma_\chi \left(d_{S,D} \right)}{\ln(P_M) + \ 2\mu_x \left(d_{S,D} \right)} + \frac{\ln(P_M) + \ 2\mu_x \left(d_{S,D} \right)}{4\sigma_\chi^2 \left(d_{S,D} \right)} \right) \sum_{i=1}^{2^N} \tilde{P}_{out-p}\left(W(i)\right)}, \tag{41}$$

where

$$\tilde{P}_{out-p}\left(W(i)\right) = \prod_{\mathrm{j}\in \mathrm{W(i)}} \Gamma(\mathrm{j})\, \frac{\sigma_\xi\left(\bar{d}_{W(i)}\right)}{\ln\left(P_M\right)+\tilde{\upsilon}\left(W(i)\right)} \left(\prod_{\mathrm{j}\notin \mathrm{W(i)}} \frac{2\sigma_\chi\left(d_{S,j}\right)}{\ln\left(P_M\right)+\ \upsilon(j)} \right) \times \exp\left(\sum_{\mathrm{j}\notin \mathrm{W(i)}} \left(-\frac{\left(\ln\left(P_M\right)+\ \upsilon(j)\right)^2}{8\sigma_\chi^2\left(d_{S,j}\right)} \right) - \frac{\left(\ln\left(P_M\right)+\tilde{\upsilon}(W(i))\right)^2}{2\sigma_\xi^2\left(\bar{d}_{W(i)}\right)} \right), \tag{42}$$

$$\hat{P}_{out-p}\left(W(i)\right) = \prod_{\mathrm{j}\in \mathrm{W(i)}} \Gamma(\mathrm{j}) \left(\frac{\ln\left(P_M\right)+\tilde{\upsilon}\left(W(i)\right)}{\sigma_\xi\left(\bar{d}_{W(i)}\right)} \Big/ \left(1+\frac{\left(\ln\left(P_M\right)+\tilde{\upsilon}\left(W(i)\right)\right)^2}{\sigma_\xi^2\left(\bar{d}_{W(i)}\right)} \right) \right) \times \prod_{\mathrm{j}\notin \mathrm{W(i)}} \left(\frac{\ln\left(P_M\right)+\upsilon\left(W(i)\right)}{\sigma_\chi\left(d_{S,j}\right)} \Big/ \left(1+\frac{\left(\ln\left(P_M\right)+\upsilon\left(W(i)\right)\right)^2}{\sigma_\chi^2\left(d_{S,j}\right)} \right) \right) \times \exp\left(\sum_{\mathrm{j}\notin \mathrm{W(i)}} \left(-\frac{\left(\ln\left(P_M\right)+\ \upsilon(j)\right)^2}{8\sigma_\chi^2\left(d_{S,j}\right)} \right) - \frac{\left(\ln\left(P_M\right)+\tilde{\upsilon}\left(W(i)\right)\right)^2}{2\sigma_\xi^2\left(\bar{d}_{W(i)}\right)} \right), \tag{43}$$

$$\hat{\kappa}(i) = \sum_{\mathrm{j}\in W(\mathrm{i})} \frac{\partial ln\Gamma(\mathrm{j})}{\partial \ln P_M} + \sum_{\mathrm{j}\in \mathrm{W(i)}} \left(\frac{\ln\left(P_M\right)+\ \upsilon(j)}{4\sigma_\chi^4\left(d_{S,j}\right)} + \frac{2\sigma_\chi\left(d_{S,j}\right)}{\ln\left(P_M\right)+\ \upsilon(j)} \right) + \frac{\ln\left(P_M\right)+\tilde{\upsilon}\left(W(i)\right)}{\sigma_\xi^2\left(\bar{d}_{W(i)}\right)} + \frac{\sigma_\xi\left(\bar{d}_{W(i)}\right)}{\ln\left(P_M\right)+\ \tilde{\upsilon}\left(W(i)\right)}, \tag{44}$$

$$\begin{aligned} \tilde{\kappa}\left(i\right) = & \sum_{\mathrm{j}\in W(i)} \frac{\partial ln\Gamma\left(\mathrm{j}\right)}{\partial \ln P_M} + \frac{\ln\left(P_M\right)+\tilde{\upsilon}\left(W\left(i\right)\right)}{\sigma_\xi^2\left(\overline{d_{W(i)}}\right)} \\ & + \left(\frac{\sigma_\xi\left(\overline{d_{W(i)}}\right)\left(\left(\ln\left(P_M\right)+\tilde{\upsilon}\left(W\left(i\right)\right)\right)^2-\sigma_\xi^4\left(\overline{d_{W(i)}}\right)\right)}{\left(\ln\left(P_M\right)+\tilde{\upsilon}\left(W\left(i\right)\right)\right)\left(\left(\ln\left(P_M\right)+\tilde{\upsilon}\left(W\left(i\right)\right)\right)^2+\sigma_\xi^4\left(\overline{d_{W(i)}}\right)\right)} \right) \\ & + \sum_{\mathrm{j}\notin W(i)} \left(\frac{2\sigma_\chi\left(d_{s,j}\right)\left(\left(\ln\left(P_M\right)+\ \upsilon\left(j\right)\right)^2-\ 4\sigma_\chi^4\left(d_{s,j}\right)\right)}{\left(\ln\left(P_M\right)+\ \upsilon\left(j\right)\right)\left(\left(\ln\left(P_M\right)+\ \upsilon\left(j\right)\right)^2+4\sigma_\chi^4\left(d_{s,j}\right)\right)} + \frac{\ln\left(P_M\right)+\ \upsilon\left(j\right)}{4\sigma_\chi^2\left(d_{s,j}\right)} \right), \end{aligned} \tag{45}$$

with $\Gamma(\mathrm{j}) = \left(1-Q\left(\left(\ln\left(P_M\right)+\ \upsilon(j)\right)/2\sigma_\chi\left(d_{S,j}\right)\right)\right)$.

Calculation of ARDO: Noting that $\Gamma(\mathrm{j}) \to 1$ if $P_M \to \infty$ and using the squeeze

theorem, ARDO is obtained by taking the limits of (40) and (41) which yields

$$ARDO = \lim_{P_M \to \infty} \frac{4\sigma_\chi^2 (d_{S,D}) \sum_{i=1}^{2^N} \tau(i) \sigma_\xi \left(\bar{d}_{W(i)}\right) \left(\prod_{\mathrm{j} \notin \mathrm{W(i)}} 2\sigma_\chi (d_{S,j}) \right) \exp\left(-\tau(i)(\ln (P_M))^2/2\right)}{\sum_{i=1}^{2^N} \sigma_\xi \left(\bar{d}_{W(i)}\right) \left(\prod_{\mathrm{j} \notin \mathrm{W(i)}} 2\sigma_\chi (d_{S,j}) \right) \exp\left(-\tau(i)(\ln (P_M))^2/2\right)} \tag{46}$$

with

$$\tau(i) = \sum_{j \notin W(i)} \left(\frac{1}{4\sigma_\chi^2 (d_{S,j})} \right) + \frac{1}{\sigma_\xi^2 \left(\bar{d}_{W(i)}\right)}. \tag{47}$$

Therefore, we finally obtain

$$ARDO = 4\sigma_\chi^2 (d_{S,D}) \min \tau(i). \tag{48}$$

Calculation of maximum achievable ARDO: To find the maximum of the ARDO of DF parallel relaying, we impose the assumption that all relays are located at the same point (see Section 3.3.2). Hence (48) can be rewritten as

$$ARDO = 4\sigma_\chi^2 (d_{S,D}) \min_{N_S(W(i))} \left(\frac{N - N_S(W(i))}{4\sigma_\chi^2 (d)} + \frac{1}{\sigma_\xi^2 (N_S(W(i)), d)} \right), \tag{49}$$

where $\sigma_\xi^2 (N_S(W(i)), d) = \ln\left(1 + \left(\exp\left(4\sigma_\chi^2 (d_{S,D} - d)\right) - 1\right)/N_S(W(i))\right)$ and $N_S(W(i))$ is the number of relays having successfully decoded the signal in the i^{th} possible decoding set, and can take values from 0 to N. If the fading variance $\sigma_\chi^2(d_{S,D} - d)$ is sufficiently small, we can approximate $\sigma_\xi^2 (N_S(W(i)), d) \approx 4\sigma_\chi^2 (d_{S,D} - d)/N_S(W(i))$. Thus, we can rewrite (49) as

$$ARDO = \sigma_\chi^2 (d_{S,D}) \min \widehat{\tau} (N_S(W(i))), \tag{50}$$

where

$$\widehat{\tau} (N_S(W(i))) = \frac{N - N_S(W(i))}{\sigma_\chi^2 (d)} + \frac{N_S(W(i))}{\sigma_\chi^2 (d_{S,D} - d)}. \tag{51}$$

For $d \leq d_{S,D}/2$, the minimum of $\widehat{\tau} (N_S(W(i)))$ occurs for $N_S(W(i)) = N$ while, for $d \geq d_{S,D}/2$, it occurs for $N_S(W(i)) = 0$. As a result, (50) can be expressed as

$$ARDO = \begin{cases} N\left(\frac{d_{S,D}}{d_{S,D} - d_{opt}}\right)^{11/6}, & d \leq d_{S,D}/2, \\ N\left(\frac{d_{S,D}}{d_{opt}}\right)^{11/6}, & d \geq d_{S,D}/2. \end{cases} \tag{52}$$

From (52), it is clear that the maximum ARDO is achieved when $d = d_{S,D}/2$. Therefore, the maximum ARDO is obtained as

$$ARDO_{max} = 2^{11/6}N. \tag{53}$$

Comparing (36) and (53), we observe that parallel relaying takes advantage of distance-dependency of fading log-normal variance to a lesser extent and is outperformed by serial relaying as the number of relays increases. We also note that (36) and (53) become equal to each other as serial and parallel relaying schemes coincide for $N = 1$.

3.5.3 Numerical Results on RDO

Fig. 5 depicts the RDO of a DF system with serial relaying for different number of relays (i.e., $N = 1, 2, 3$). We consider a log-normal turbulence channel with standard deviations of $\sigma_x(d_{S,D}) = 0.1$ and $\sigma_x(d_{S,D}) = 0.3$ along with the other assumptions about system and channel conditions detailed in Section 3.4. Assuming $P_M = 100$ dB, we observe RDO values of 3.7, 7.9 and 13.5 respectively for $N = 1, 2$ and 3. These provide a good match to analytical ARDOs (i.e., $P_M \to \infty$) calculated as $(N+1)^{11/6} = 3.6, 7.5$, and 12.7 respectively for $N = 1$, 2 and 3. We also observe that RDOs for lower P_M values are higher than those for higher P_M. This can be explained by the success of serial relaying in reduction of path loss effects which are more pronounced in lower transmit power regions.

Fig. 6 demonstrates the RDO of a DF system with parallel relaying for $N = 2$ and 3[1]. As clearly seen, particularly for small values of fading variance, substantial improvement in RDO is achieved when the relays are located at the optimum position instead of simply being located at the halfway point. At $P_M = 100$ dB, we observe RDO values of 7.17, and 10.6 for $N = 2$ and 3. These values are very close to analytical ARDOs (i.e. $P_M \to \infty$) which are obtained as $2^{11/6}N = 7.12$, and 10.7 for $N = 2$ and 3 confirming our analytical derivations.

[1]Note that for $N = 1$, serial and parallel relaying schemes coincide.

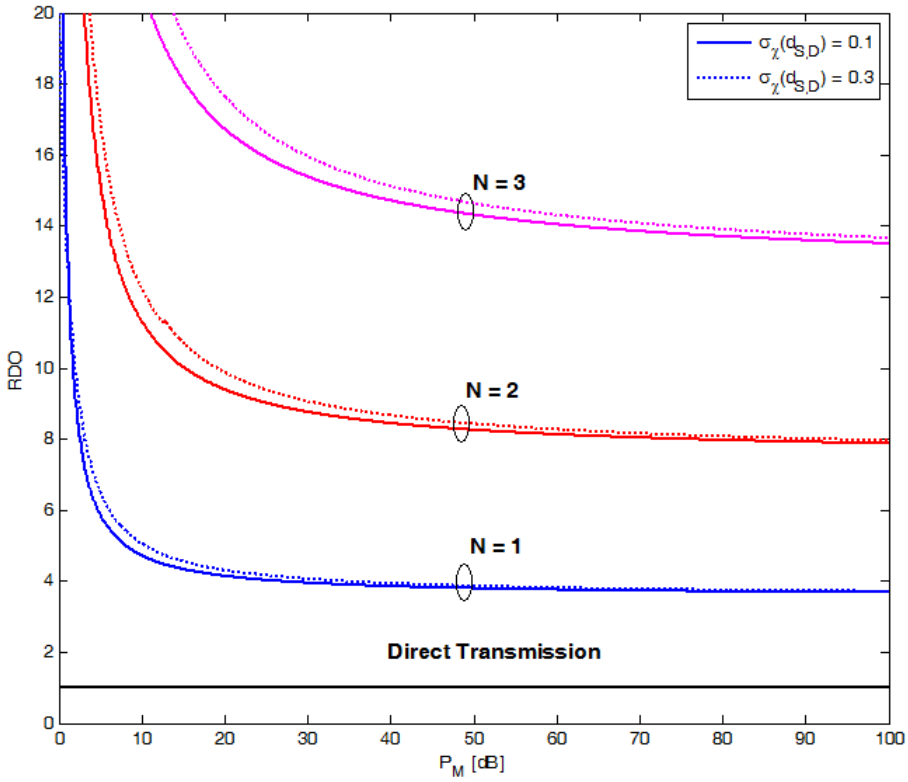

Figure 5: RDO of serial FSO relaying scheme for different number of relays.

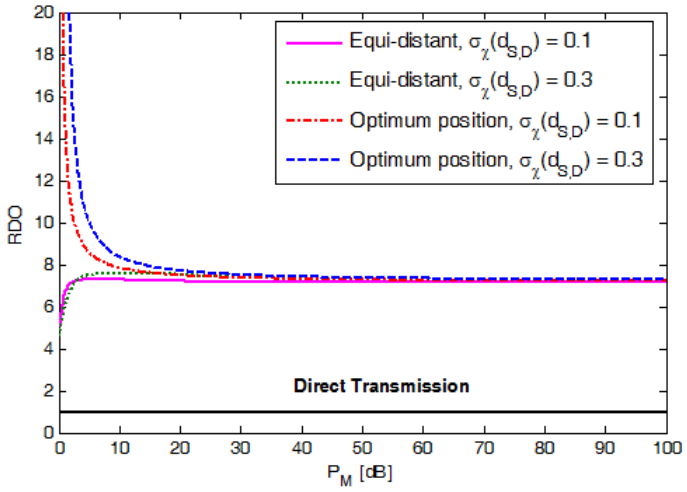

(a)

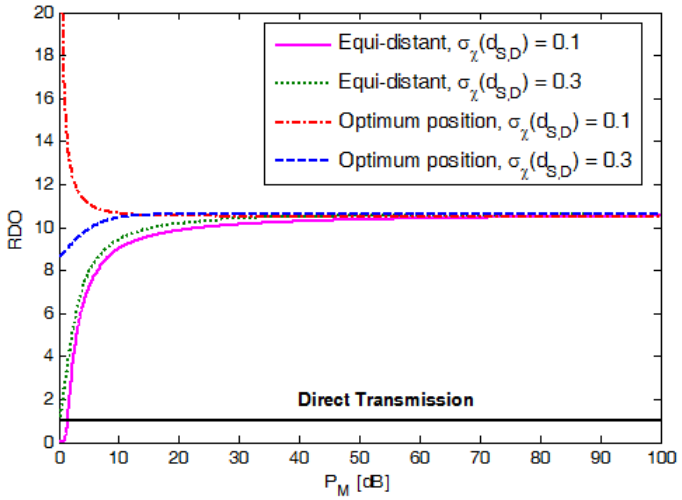

(b)

Figure 6: RDO of parallel FSO relaying scheme for a) two relays, and b) three relays.

CHAPTER IV

MULTI-HOP PARALLEL FSO RELAYING

Since FSO is a line-of-sight technology, a practical FSO mesh network would be likely to deploy a combination of serial and parallel relaying. In this part, we extend the results of [28] to this general and more practical scenario and derive the outage performance of a *multi-hop parallel* DF FSO network. Our outage probability analysis demonstrates substantial performance improvements with respect to both stand-alone serial and parallel relaying schemes. Furthermore, we present a diversity gain analysis and quantify the achievable diversity order in terms of the number of relays and the turbulence channel parameters.

4.1 System Model

We consider a multi-hop parallel FSO communication system illustrated in Fig. 7. We assume that there is a source node which communicates with a destination node via the total of N relays. Nearby relays are grouped together resulting in a number of K groups. Let N_i, $i = 1, 2, \ldots K$, denote the number of relay nodes in the i^{th} group. The source node is equipped with a multi-laser transmitter and each of the transmitter points out in the direction of a corresponding relay node within the first group. The number of the relays at the i^{th} group might be less than the number of the relays at $(i-1)^{th}$ group, i.e., $N_i < N_{i-1}$. Therefore, all the relays (except those in the first group) and the destination are supposed to have a sufficiently large aperture that allows the simultaneous detection of several optical fields transmitted from different relay nodes of the previous group.

We assume the deployment of BPPM. Transmission takes place in $K+1$ phases. In the first phase, the source transmits the same BPPM signal to N_1 relay nodes (i.e., the

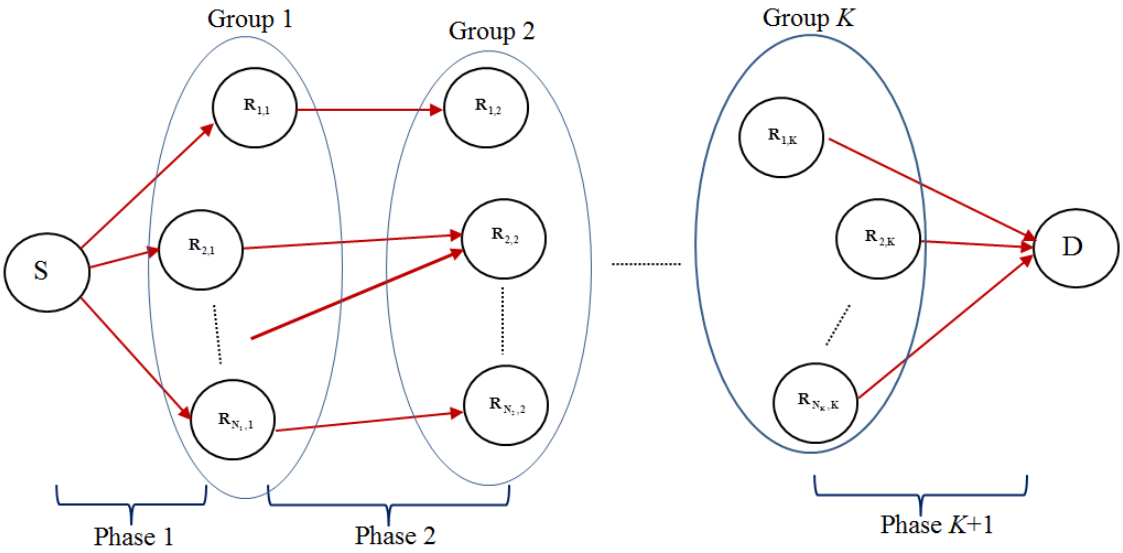

Figure 7: Multi-hop parallel FSO relaying network.

first group of relays). In the next phase, each relay, after direct detection, modulates it with BPPM and retransmits the signal to the next group and this continues until the source's data arrives at the destination node. We assume the deployment of so-called "selective" DF relaying [47] in which a relay is engaged in forwarding only if its received SNR exceeds a given decoding threshold. Otherwise, to avoid error propagation, it remains silent.

In selective DF relaying, we refer the relay nodes which are engaged in forwarding as *active relays*. The set of active relays at the i^{th} group is named as active relay set and denoted by W_i. Furthermore, we denote the *successful relay set* by D_i, i.e., the set of active relays in W_i having successfully decoded the signal. Therefore, there exists $2^{|W_i|}$[1] possible forms for the successful set at the i^{th} phase, $i = 1, 2, \ldots K$.

Let D_{i-1}^{k} denote the set of relays within the i^{th} successful set pointing out in the direction of the k^{th} node (denoted by k_i) within the i^{th} successful group. The received

[1] $|W_i|$ denotes the cardinality of W_i and therefore represents the number of the active relays in the i^{th} group.

signal at the k_i^{th} relay is therefore given by

$$\mathbf{r}_{k_1} = \begin{bmatrix} r_{k_1}^s \\ r_{k_1}^n \end{bmatrix} = \begin{bmatrix} RT_b \left(P_a A_{S,k_1} + P_b \right) + n_{k_1}^s \\ RT_b P_b + n_{k_1}^n \end{bmatrix}, \tag{54a}$$

$$\mathbf{r}_{k_i} = \begin{bmatrix} r_{k_i}^s \\ r_{k_i}^n \end{bmatrix} = \begin{bmatrix} RT_b \left(P_a \sum\limits_{j_{i-1} \in D_{i-1}^k} A_{j_{i-1},k_i} + P_b \right) + n_{k_i}^s \\ RT_b P_b + n_{k_i}^n \end{bmatrix}, \tag{54b}$$

where $r_{k_i}^s$ and $r_{k_i}^n$, respectively, denote the received signal and non-signal slots of the BPPM pulse. In (54), P_b is the background power incident on the photodetector, P_a denotes the average transmitted optical power per transmit aperture and is related to the total transmitted power (P_t) by $P_a = P_t/\kappa$ where $\kappa = N + N_1$ is the total number of the transmit apertures in the relaying configuration. $n_{k_i}^s$ and $n_{k_i}^n$ in (54) denote the additive noise terms respectively for the signal and the non-signal slots. We assume that the intensity of the light incident on the photodetector is sufficiently high. In this case, the shot noise caused by background radiation is dominant. Therefore, a signal-independent additive white Gaussian noise with zero mean and variance of $\sigma_{n_{K_i}}^2 = \eta_0/2$ can accurately approximate the Poisson photon-counting detection model [3].

4.2 Outage Probability Analysis

Recall that for the multi-hop parallel relaying scheme under consideration, the successful relay set at the i^{th} phase, $i = 1, 2, \ldots K$, has $2^{|W_i|}$ possibilities. Let $U_i(j)$ denote the j^{th} possible set for D_i. Furthermore, let $\bar{d}_{U_i(j),n}$ denote the set of all distances between the n^{th} active node in the $(i+1)^{th}$ group and the successful relays in the i^{th} active relay set pointing out in the direction of the corresponding relay node, i.e.,$d_{m,n} \in \bar{d}_{U_i(j),n}$, $m \in U_i(j)$, $1 \leq n \leq |W_{i+1}|$.

In multi-hop parallel relaying, an outage occurs if either none of the active relay nodes decodes the signal successfully or multiple-input single-output link in the last

phase fails. The corresponding outage probability can be then given by

$$P_{out} = \sum_{i_1=1}^{2^{N_1}} P_{out,phase_2}\ \left(U_1\left(i_1\right)\right) \Pr\left(U_1\left(i_1\right)\right). \tag{55}$$

In (55), $P_{out,phase_2}\left(U_1\left(i_1\right)\right)$ is the outage probability of the second phase during which the successful relays involved in the event $\{D_1 = U_1\left(i_1\right)\}$ retransmit signal to the corresponding relay nodes of the second group. In (55), $\Pr\left(U_1\left(i_1\right)\right)$ denotes the probability of the event $\{D_1 = U_1\left(i_1\right)\}$ and is given by

$$\begin{aligned}\Pr\left(U_1\left(i_1\right)\right) &= \Pr\left[\left(\bigcap\nolimits_{m_1 \in U_1(i_1)} m_1 \in U_1\left(i_1\right)\right) \bigcap \left(\bigcap\nolimits_{m_1 \notin U_1(i)} m_1 \notin U_1\left(i_1\right)\right)\right] \\ &= \prod_{m_1 \in U_1(i_1)} \left(1 - P_{out,SISO}\left(d_{S,m_1}\right)\right) \prod_{m_1 \notin U_1(i_1)} P_{out,SISO}\left(d_{S,m_1}\right),\end{aligned} \tag{56}$$

where $P_{out,SISO}\left(d_{S,m_1}\right)$ is the outage performance of the intermediate single-input single-output link connecting the source and the m_1^{th} node. Its derivation can be found in Eq. (21) of [28].

Let $P_{out,MISO}\left(\bar{d}_{U_{j-1}(i_{j-1}),m_j}\right)$ denote the outage performance of the MISO link between the successful relays in the $U_{j-1}\left(i_{j-1}\right)$ successful relay set and the m_j^{th} node. Its closed form expression is given by Eq. (29) of [28]. The outage probability of the j^{th} phase $(j = 2, 3, \ldots, K)$ corresponding to the event $\{D_{j-1} = U_{j-1}\left(i_{j-1}\right)\}$ can be then expressed as

$$P_{out,phase_j}\left(U_{j-1}\left(i_{j-1}\right)\right) = \sum_{i_j\ =1}^{2^{\left|W_j\right|}} P_{out,phase_{j+1}}\left(U_j\left(i_j\right)\right) \Pr\left(U_j\left(i_j\right)\right) \tag{57}$$

with

$$\Pr\left(U_j\left(i_j\right)\right) = \prod_{m_j \in U_j(i_j)} \left(1 - P_{out,MISO}\left(\bar{d}_{U_{j-1}(i_{j-1}),m_j}\right)\right) \prod_{m_j \notin U_j(i_j)} P_{out,MISO}\left(\bar{d}_{U_{j-1}(i_{j-1}),m_j}\right). \tag{58}$$

Therefore, we can rewrite (55) as

$$P_{out} = \sum_{i_1=1}^{2^{N_i}} \Pr\left(U_1\left(i_1\right)\right) \sum_{i_2=1}^{2^{|W_2|}} \Pr\left(U_2\left(i_2\right)\right) \cdots \sum_{i_K=1}^{2^{|W_K|}} \Pr\left(U_K\left(i_K\right)\right) P_{out,MISO}\left(\bar{d}_{U_K(i_K),D}\right). \tag{59}$$

Let us define the following functions

$$H\left(d_{i,j}\right) \overset{def}{=} Q\left(\frac{\ln\left(L\left(d_{i,j}\right) P_M/\kappa\ \right) + 2\mu_\chi\left(d_{i,j}\right)}{2\sigma_\chi\left(d_{i,j}\right)}\right), \tag{60}$$

$$G(\bar{d}) \overset{def}{=} Q\left(\frac{\ln\left(P_M/\kappa\ \right) + \mu_\xi\left(\bar{d}\right)}{\sigma_\xi\left(\bar{d}\right)}\right). \tag{61}$$

$\mu_\xi\left(\bar{d}\right)$ and $\sigma_\xi\left(\bar{d}\right)$ in (60) and (61) can be respectively found in (9) and (10). Inserting the equations (56) and (58) in (59), the outage probability for multi-hop parallel scheme is obtained as

$$\begin{aligned}
P_{out} &= \sum_{i_1=1}^{2^{N_1}} P_{out-1}\left(U_1\left(i_1\right)\right) \qquad (62)\\
&= \sum_{i_1=1}^{2^{N_1}} \prod_{m_1 \in U_1(i_1)} \left(1 - H\left(d_{S,m_1}\right)\right) \prod_{m_1 \notin U_1(i_1)} H\left(d_{S,m_1}\right)\\
&\times \sum_{i_2=1}^{2^{|W_2|}} \prod_{m_2 \in U_2(i_2)} \left(1 - G\left(\bar{d}_{U_1(i_1),m_2}\right)\right) \prod_{m_2 \notin U_2(i_2)} G\left(\bar{d}_{U_1(i_1),m_2}\right) \cdots\\
&\times \sum_{i_j=1}^{2^{|W_j|}} \prod_{m_j \in U_j(i_j)} \left(1 - G\left(\bar{d}_{U_{j-1}(i_{j-1}),m_j}\right)\right) \prod_{m_j \notin U_j(i_j)} G\left(\bar{d}_{U_{j-1}(i_{j-1}),m_j}\right) \cdots\\
&\times \sum_{i_K=1}^{2^{|W_K|}} \prod_{m_K \in U_K(i_K)} \left(1 - G\left(\bar{d}_{U_{K-1}(i_{K-1}),m_K}\right)\right) \prod_{m_K \notin U_K(i_K)} G\left(\bar{d}_{U_{K-1}(i_{K-1}),m_K}\right) G\left(\bar{d}_{U_K(i_K),D}\right).
\end{aligned}$$

Special cases: The derived expression for the multi-hop parallel relaying includes the earlier derived results in [28] as special cases. First, assume $N = K$ which corresponds to the case of serial (multi-hop) transmission. Under this assumption, (62) reduces to

$$\begin{aligned}
&P_{out-Serial} = H\left(d_{S,m_1}\right) + \left(1 - H\left(d_{S,m_1}\right)\right) H\left(d_{m_1,m_2}\right) + ...\\
&+ \left(1 - H\left(d_{S,m_1}\right)\right)\left(1 - H\left(d_{m_1,m_2}\right)\right) \times ... \times \left(1 - H\left(d_{m_{K-2},m_{K-1}}\right)\right) H\left(d_{m_{K-1},m_K}\right).
\end{aligned} \tag{63}$$

This can be further rewritten as

$$\begin{aligned}
P_{out-Serial} &= 1-\left(1-H\left(d_{S,m_1}\right)\right)+\left(1-H\left(d_{S,m_1}\right)\right)H\left(d_{m_1,m_2}\right)+... \\
&+\left(1-H\left(d_{S,m_1}\right)\right)\left(1-H\left(d_{m_1,m_2}\right)\right)\times...\times\left(1-H\left(d_{m_{K-1},m_K}\right)\right)H\left(d_{m_K,D}\right) \\
&=1-\left(1-H\left(d_{S,m_1}\right)\right)H\left(d_{m_K,D}\right)\prod_{i=1}^{K-1}\left(1-H\left(d_{m_i,m_{i+1}}\right)\right),
\end{aligned} \tag{64}$$

which coincides with (24) of [28].

Now, assume$K=1$ which corresponds to the case of parallel relaying. Under this assumption, (62) reduces to

$$P_{out-Parallel}=\sum_{i_1=1}^{2^N}\left[\prod_{m_1\in U_1(i_1)}\left(1-H\left(d_{S,m_1}\right)\right)\prod_{m_1\notin U_1(i_1)}H\left(d_{S,m_1}\right)\right]G\left(\bar{d}_{U_1(i_1),D}\right), \tag{65}$$

which coincides with (32) of [28].

4.3 Diversity Gain Analysis

The RDO of multi-hop parallel relaying scheme under consideration is obtained as

$$\mathrm{RDO}(P_M)=\frac{\partial\ln\left(\sum_{i_1=1}^{2^{N_1}}P_{out-1}\left(U_1\left(i_1\right)\right)\right)/\partial\ln P_M}{\partial\ln\left(Q\left(\left(\ln\left(P_M\right)+2\mu_\chi\right)/2\sigma_\chi\right)\right)/\partial\ln P_M}. \tag{66}$$

The numerator of (66) can be rearranged as

$$F=\frac{\sum_{i_1=1}^{2^{N_1}}\frac{\partial P_{out-1}(U_1(i_1))}{\partial\ln P_M}}{\sum_{i_1=1}^{2^{N_1}}P_{out-1}\left(U_1\left(i_1\right)\right)}. \tag{67}$$

Let us define P_{out-j}, $j=2,3,...,K$ as

$$\begin{aligned}
P_{out-j}=&\sum_{i_j=1}^{2^{|W_j|}}\prod_{m_j\in U_j(i_j)}\left(1-G\left(\bar{d}_{U_{j-1}(i_{j-1}),m_j}\right)\right)\prod_{m_j\notin U_j(i_j)}G\left(\bar{d}_{U_{j-1}(i_{j-1}),m_j}\right)\cdots \\
\times&\sum_{i_K=1}^{2^{|W_K|}}\prod_{m_K\in U_K(i_K)}\left(1-G\left(\bar{d}_{U_{K-1}(i_{K-1}),m_K}\right)\right)\prod_{m_K\notin U_K(i_K)}G\left(\bar{d}_{U_{K-1}(i_{K-1}),m_K}\right)G\left(\bar{d}_{U_K(i_K),D}\right).
\end{aligned} \tag{68}$$

Differentiation with respect to $\ln P_M$ yields

$$\frac{\partial P_{out-j}}{\partial \ln P_M} = \frac{\sum_{i_j=1}^{2^{|W_j|}} P_{out-j} \left(\partial \upsilon_j / \partial \ln P_M \ + \left(\partial \ln P_{out-j+1} / \partial \ln P_M \ \right)\right)}{\sum_{i_j=1}^{2^{|W_j|}} P_{out-j}}, \tag{69}$$

where υ_1 , υ_j $j = 2, 3, \ldots, K-1$ and υ_K are respectively defined as

$$\upsilon_1 = \sum_{m_1 \in U_1(i_1)} \ln\left(1 - H\left(d_{S,m_1}\right)\right) + \sum_{m_1 \notin U_1(i_1)} \ln\left(H\left(d_{S,m_1}\right)\right) \tag{70}$$

$$\upsilon_j = \sum_{m_j \in U_j(i_j)} \ln\left(1 - G\left(\bar{d}_{U_{j-1}(i_{j-1}),m_j}\right) \ \right) + \sum_{m_j \notin U_j(i_j)} \ln\left(G\left(\bar{d}_{U_{j-1}(i_{j-1}),m_j}\right)\right) \tag{71}$$

$$\begin{aligned}\upsilon_K = &\sum_{m_K \in U_K(i_K)} \ln\left(1 - G\left(\bar{d}_{U_{K-1}(i_{K-1}),m_K}\right)\right) + \ln\left(G\left(\bar{d}_{U_K(i_K),D}\right) \ \right) \\ &+ \sum_{m_K \notin U_K(i_K)} \ln\left(G\left(\bar{d}_{U_{K-1}(i_{K-1}),m_K}\right)\right)\end{aligned} \tag{72}$$

Employing the bounds on Q function which is given by (28) and the squeeze theorem, ARDO can be obtained by taking the limit of (66) as

$$\begin{aligned}ARDO = 4\sigma_\chi^2\left(d_{S,D}\right) &\min_{U_1(i_1)} \left(\sum_{m_1 \notin U_1(i_1)} \left(\frac{1}{4\sigma_\chi^2\left(d_{S,m_1}\right)} \right) \right. \\ + \min_{U_2(i_2)} &\left(\sum_{m_2 \notin U_2(i_2)} \left(\frac{1}{\sigma_\xi^2\left(\bar{d}_{U_1(i_1),m_2}\right)} \right) + \cdots + \min_{U_j(i_j)} \left(\sum_{m_j \notin U_j(i_j)} \left(\frac{1}{\sigma_\xi^2\left(\bar{d}_{U_{j-1}(i_{j-1}),m_j}\right)} \right) \right. \right. \\ + \cdots + \min_{U_K(i_K)} &\left. \left. \left. \left(\sum_{m_K \notin U_K(i_K)} \frac{1}{\sigma_\xi^2\left(\bar{d}_{U_{K-1}(i_{K-1}),m_K}\right)} + \frac{1}{\sigma_\xi^2\left(\bar{d}_{U_K(i_K),D}\right)} \right) \right) \right) \cdots \right).\end{aligned} \tag{73}$$

For a sanity check, we consider some special cases in the following. Let us *hypothetically* assume that each of the groups consists the same number of relays which can detect only one signal[1], and each group is equidistant along the path from the source

[1]This is a special case of the original assumption where we consider that all the relays (except those in the first group) have a sufficiently large aperture allowing the simultaneous detection of several signals.

to the destination[1]. Under these assumptions, we can rewrite (73) as

$$ARDO = 4\sigma_\chi^2\left(d_{S,D}\right) \min_{|U_1(i_1)|}\left(\frac{N/K - |U_1\left(i_1\right)|}{4\sigma_\chi^2\left(d_{S,D}/(K+1)\right)}\right.$$
$$+ \min_{|U_2(i_2)|}\left(\frac{|U_1\left(i_1\right)| - |U_2\left(i_2\right)|}{4\sigma_\chi^2\left(d_{S,D}/(K+1)\right)} + \cdots + \min_{|U_j(i_j)|}\left(\frac{|U_{j-1}\left(i_{j-1}\right)| - |U_j\left(i_j\right)|}{4\sigma_\chi^2\left(d_{S,D}/(K+1)\right)} + \cdots\right.\right.$$
$$\left.\left.\left. + \min_{|U_K(i_K)|}\left(\frac{|U_{K-1}\left(i_{K-1}\right)| - |U_K\left(i_K\right)|}{4\sigma_\chi^2\left(d_{S,D}/(K+1)\right)} + \frac{1}{\sigma_\xi^2\left(|U_K\left(i_K\right)|, d_{S,D}/(K+1)\right)}\right)\right)\right), \quad (74)$$

where $|U_j\left(i_j\right)|$ stands for the cardinality of $U_j\left(i_j\right)$ and therefore is the number of relays in the i_j^{th} possible set for the j^{th} successful relay set (i.e., $\mathrm{D_j}$) and $\sigma_\xi^2\left(|U_K\left(i_K\right)|, d_{S,D}/(K+1)\right)$ is given by

$$\sigma_\xi^2\left(|U_K\left(i_K\right)|, d_{S,D}/(K+1)\right) = \ln\left(1 + \left(\exp\left(4\sigma_\chi^2\left(d_{S,D}/(K+1)\right)\right) - 1\right)/\left|U_K\left(i_K\right)\right|\right). \quad (75)$$

If the fading variance $\sigma_\chi^2\left(d_{S,D}/(K+1)\right)$ is sufficiently small, we can approximate

$$\sigma_\xi^2\left(|U_K\left(i_K\right)|, d_{S,D}/(K+1)\right) \approx 4\sigma_\chi^2\left(d_{S,D}/(K+1)\right)/\left|U_K\left(i_K\right)\right|. \quad (76)$$

Thus, we finally obtain

$$ARDO = (K+1)^{11/6}\frac{N}{K}. \quad (77)$$

If $K = N$, we have

$$ARDO = (N+1)^{11/6}, \quad (78)$$

which is the case of serial relaying given by (36). On the other hand, if we set $K = 1$, we have

$$ARDO = 2^{11/6}N, \quad (79)$$

which is the case of parallel relaying given by (53).

4.4 Numerical Results

In this section, we present numerical results for the derived outage performance expressions. We consider the same assumptions about system and channel conditions

[1]This assumption requires that all of the relays in each group are located at the same location.

detailed in Section 3.4. In the following, we assume a total of $N = 6$ relays and present the outage performance for a number of different configurations:

- **Configuration 1 (C1)**: In this configuration, we have three groups of relays (i.e., $K = 3$) and each of them consists 2 relays (i.e., $N_1 = N_2 = 2$)
- **Configuration 2 (C2)**: In this configuration, we have two groups of relays (i.e., $K = 2$) and each of them consists 3 relays (i.e., $N_1 = N_2 = 3$)
- **Configuration 3 (C3)**: In this configuration, we have a single group of 6 relays located at the vertical line of the midway point between the source and the destination.

These configurations based on the mix use of parallel and multi-hop relaying are illustrated in Fig. 8. As benchmarks, we also consider some configurations in which only the use of either parallel or multi-hop relaying is allowed for the same number of relays. Specifically, Fig. 9.a. and 9.b. respectively illustrate the multi-hop and parallel relaying schemes for $K = 3$ and $N_1 = N_2 = 2$. These will be used as benchmarks for C1. Similarly, Fig. 10.a. and 10.b. respectively illustrate the multi-hop and parallel relaying schemes which will be used as benchmarks for C2. Fig. 11 illustrates the benchmarking multi-hop scheme for C3.

Figs. 12 and 13 present the outage performance of C1 and C2 with the aforementioned benchmarks. As clearly seen from these figures, the combined use of parallel and multi-hop relaying substantially improves the performance with respect to stand-alone uses of multi-hop and parallel relaying. Particularly, for an outage probability of 10^{-6}, we observe performance improvements of 6.8 dB and 9.8 dB for $K = 2$ and 3 with respect to stand-alone parallel relaying. On the other hand, with respect to stand-alone serial relaying, performance gains of 3.8 dB and 9.2 dB are respectively observed for $K = 2$ and 3. It should be noted that these performance gains are a

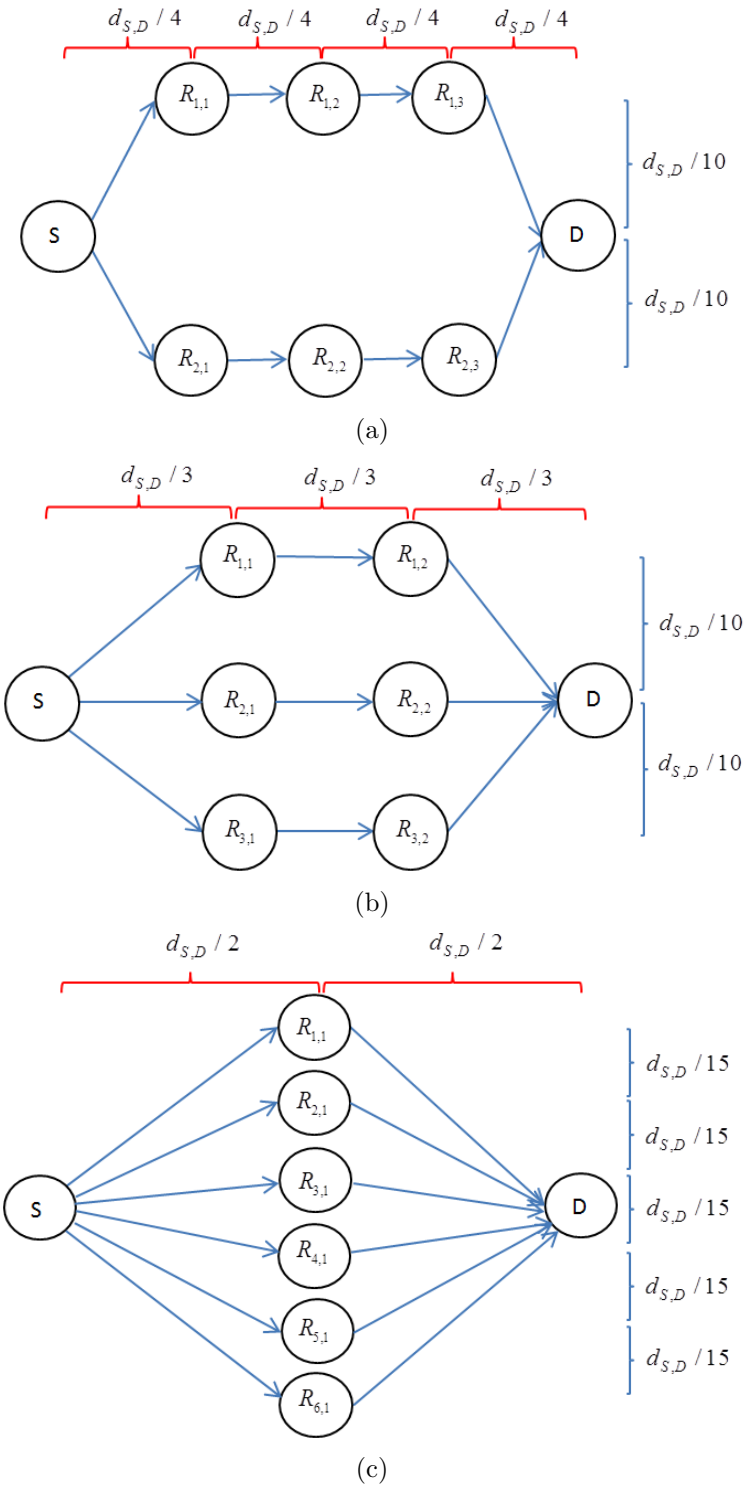

Figure 8: Configurations under consideration a) C1: three groups of relays, b) C2: two groups of relays, and c) C3: single group of relays

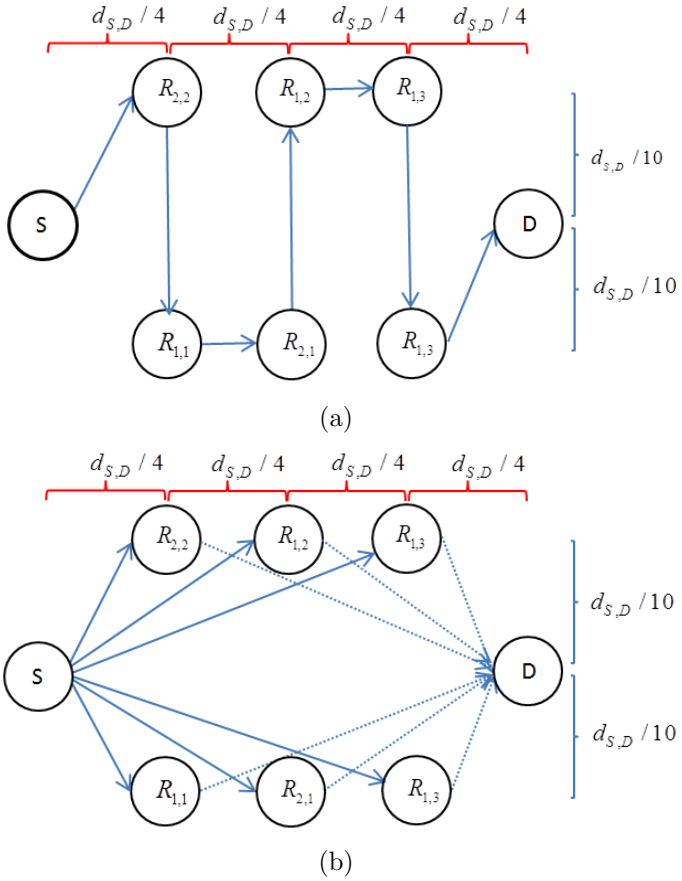

Figure 9: a) Multi-hop and b) Parallel relaying benchmarking schemes for C1.

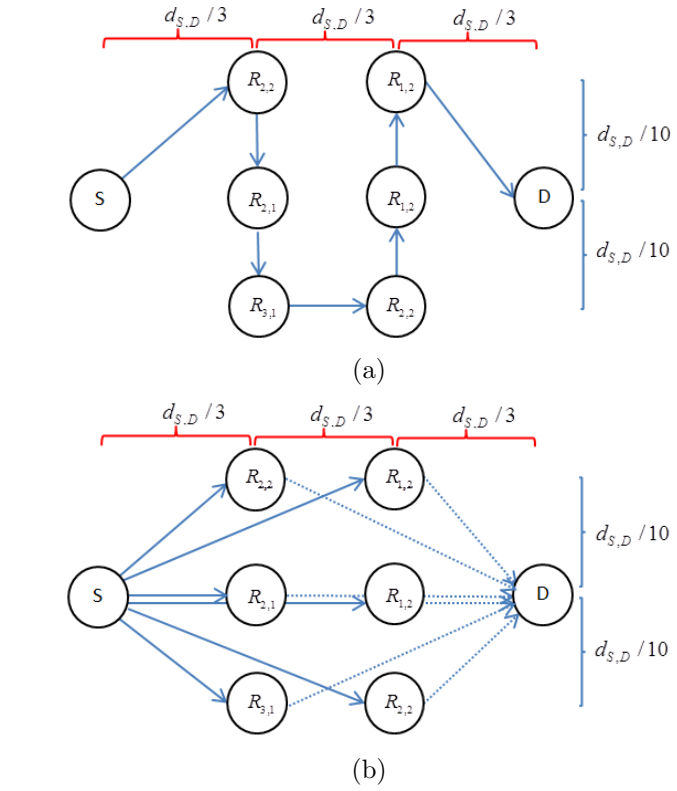

Figure 10: a) Multi-hop and b) Parallel relaying benchmarking schemes for C2.

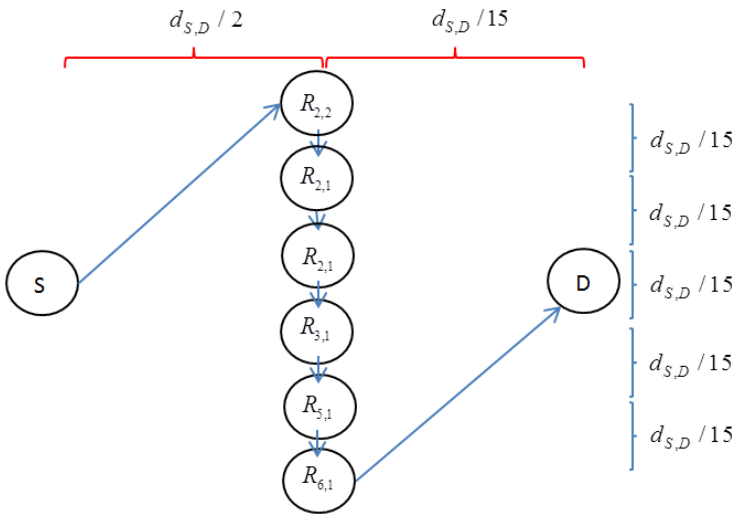

Figure 11: Multi-hop relaying benchmarking scheme for C3.

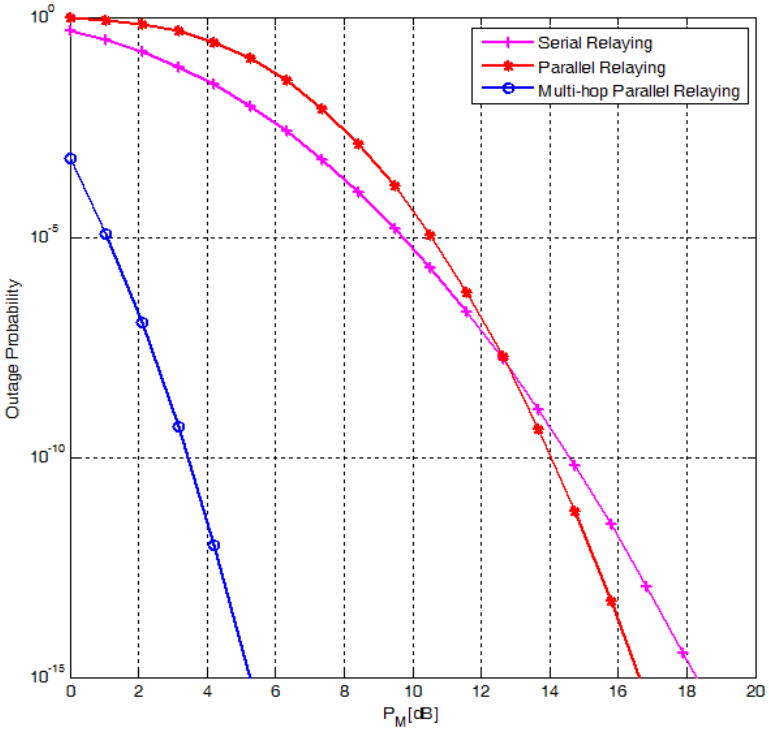

Figure 12: Performance comparison of multi-hop parallel, serial and parallel relaying for C1.

result of the nature of multi-hop parallel relaying which smartly exploits the distance-dependency of the log-amplitude variance more than the stand-alone versions.

In Fig. 14, the outage performance of C3 along with the benchmark is illustrated. We note that for $K = 1$ the performance of parallel and multi-hop parallel relaying coincide as expected. For a target outage probability of 10^{-6}, this configuration achieves a performance improvement of 8.3 dB with respect to the stand-alone version.

In Fig. 15, we compare the performance of C1, C2 and C3 and investigate the effect of the number of groups for a fixed number of relays. We observe from 15 that increasing the number of groups results in performance improvement. For a target outage probability of 10^{-6}, the performance gains for $K = 3$ are 7.5 dB and 2.9 dB with respect to $K = 1$ and 2. This is as a result of increasing hops exploiting the distance-dependency of the log-amplitude variance to a greater extent.

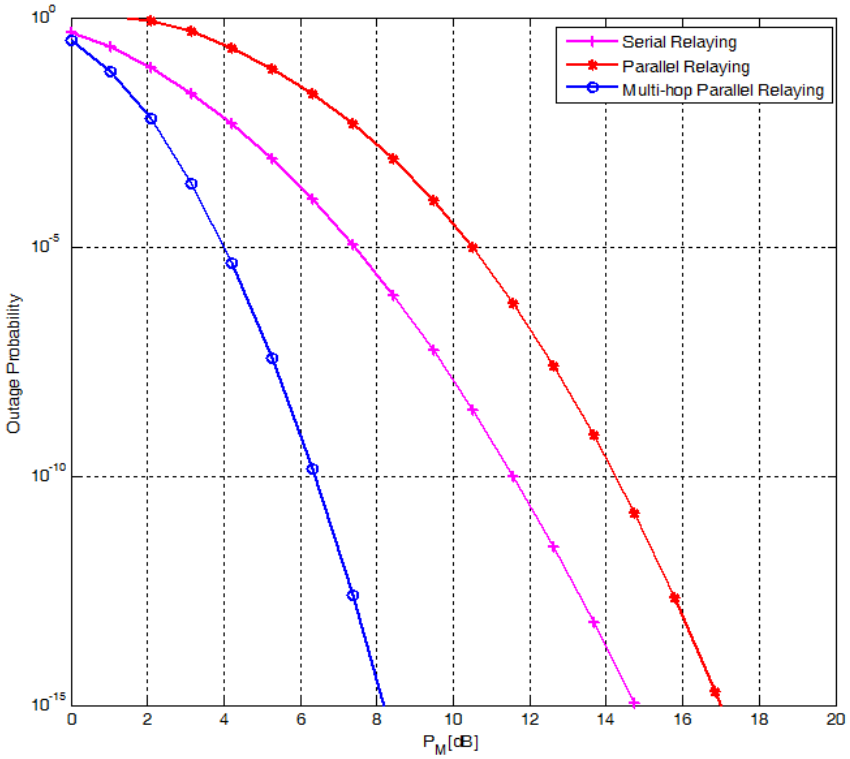

Figure 13: Performance comparison of multi-hop parallel, serial and parallel relaying for C2.

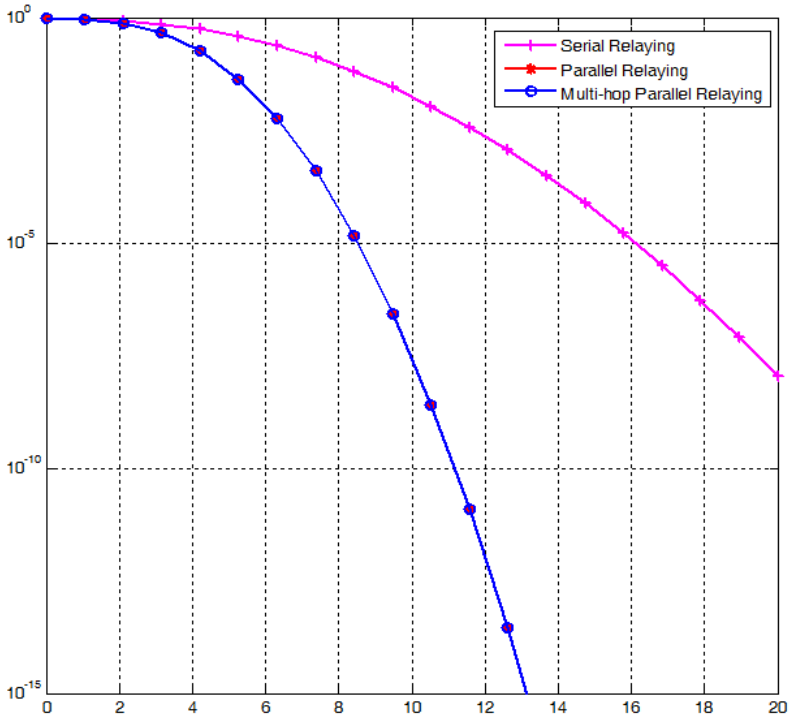

Figure 14: Performance comparison of multi-hop parallel, serial and parallel relaying for C3.

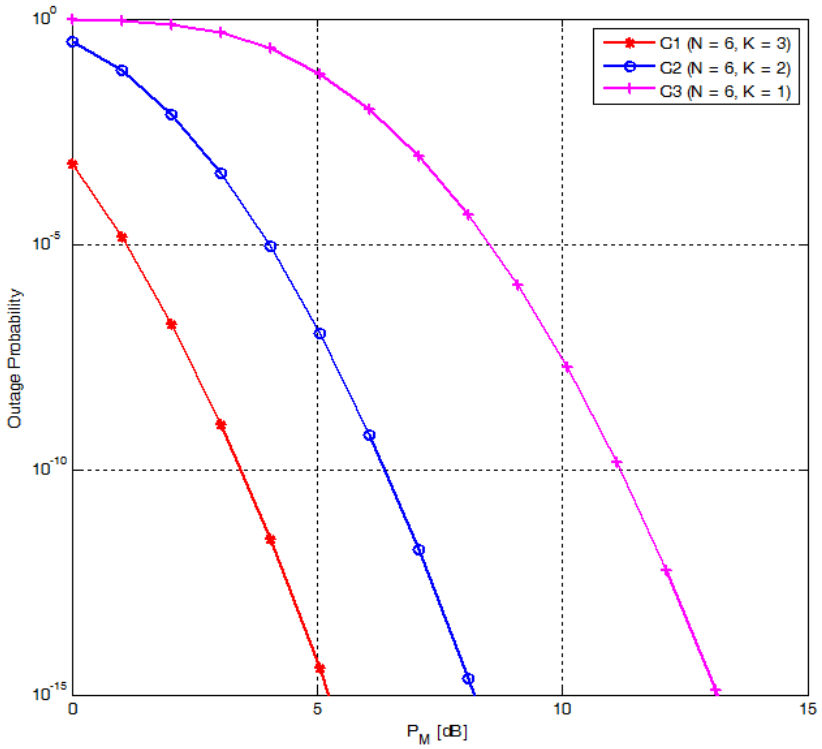

Figure 15: Effect of different number of groups on the outage performance.

Finally, Fig. 16 depicts the RDO values of C1, C2 and C3 under consideration. For $P_M \to$ 100 dB, we observe RDO values of 24, 22.2 and 19.7 respectively for C1, C2 and C3. These perfectly match to the ARDOs in (73) and are in good agreement with the simplified ARDOs in (77) calculated as $(K+1)^{11/6}N/K = 25.4$, 22.5 and 21.4.

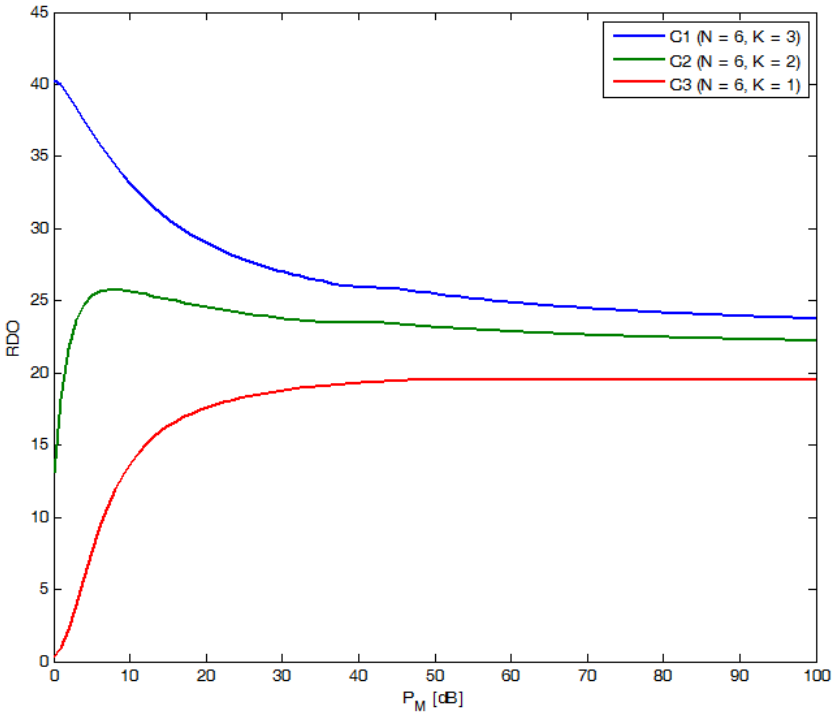

Figure 16: RDO values for C1, C2 and C3.

CHAPTER V

ALL-OPTICAL AMPLIFY-AND-FORWARD RELAYING SYSTEM FOR ATMOSPHERIC CHANNELS

The current literature on AF relaying in FSO systems [26, 28, 36, 37] builds on the assumption that relays employ optical-electrical and electrical-to-optical convertors. The actual advantage of AF relaying over the DF counterpart emerges if its implementation avoids the requirement for high-speed (at the order of GHz) electronics and electro-optics. This becomes possible with *all-optical* AF relaying where the signals are processed in optical domain and such relays require only low-speed electronic circuits to control and adjust the gain of amplifiers [38]. Therefore, EO/OE domain conversions are eliminated, allowing efficient implementation.

All-optical AF relaying has been considered in recent papers [48, 49]. In particular, Kazemlou *et al.* [48] have assumed either fixed-gain optical amplifiers or optical regenerator, and presented bit error rate (BER) performance through Monte Carlo simulations. Their work does not take into account the effect of amplified spontaneous emission noise (ASE) noise. On the other hand, in [49] Bayaki *et al.* have considered all-optical relays employing erbium-doped fiber amplifiers (EDFAs) and presented an outage probability analysis for a dual-hop system. However, in their paper, they have not considered the effect of the optical degree-of-freedom (DoF).

In this chapter, we consider an FSO system with all-optical AF relaying and investigate its outage performance taking into account the effects of ASE and DoF. ASE is the main source of noise in doped fiber amplifiers (DFAs) and will inevitably affect the performance of a relay. For example, noise figure in an ideal DFA is 3 dB, while practical amplifiers can have noise figure as large as 6-8 dB [50]. On the other

hand, DoF quantifies the ratio of optical filter bandwidth to the electrical bandwidth and can be on the order of 1000 unless narrowband optical filtering is employed [51]. For the sake of presentation, we restrict our performance analysis in this letter to a single-relay scenario (i.e., dual hop), but extension to multiple hops is straightforward. We derive closed form expressions for the outage probability assuming either full channel state information (CSI) or only statistical CSI. We present numerical results to compare the performance of so-called *full-CSI* and *semi-blind* relays and demonstrate the effect of DoF on the outage performance.

5.1 System Model

We consider a dual-hop IM/DD FSO transmission system with binary pulse position modulation (BPPM). The source terminal modulates and transmits the intensity-modulated signal. At the relay terminal (see Fig. 17), the received signals are optically filtered and amplified. In practice, erbium doped fiber amplifiers (EDFAs) are typically employed for signal amplification. By cascading a series of EDFAs, the relay can sweep its gain over a wide range. Both pre- and post-filtering are utilized to minimize the effects of background noise and ASE of optical amplifier(s). In full-CSI relaying case, instantaneous CSI of the source-to-relay link is assumed to be available at the relay and is used for the calculation of the amplification gain before retransmission of the received signal. On the other hand, in semi-blind relaying case, only statistical CSI (i.e., knowledge of the average fading power) is available; therefore a fixed coefficient is used in the amplification process. The optical signal is then redirected to the destination terminal. EDFAs are used at the destination to overcome the limitations of electrical noise at high data rates mainly dominated by the thermal noise. Under the assumption of a high gain EDFA ($\sim$ 30 dB) at the destination, we consider a shot-noise limited system in which the effect of thermal noise can be neglected and only shot noise caused by background radiation is dominant. Therefore,

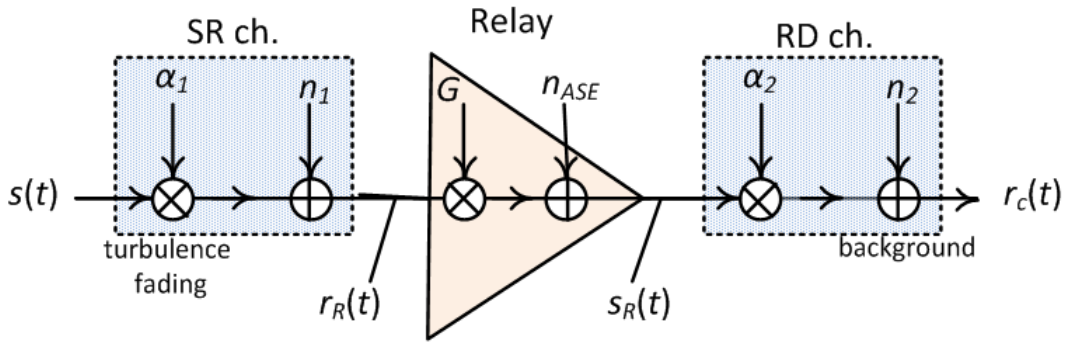

Figure 17: Block diagram of an all-optical relay terminal.

the noise at the destination is modeled by additive noise.

Let us assume that source terminal transmits photons with rate $s(t)$ (with an average of m_1) which obeys a Poisson distribution. The photon rate at the relay can be expressed as [52]

$$r_R(t) = \alpha_1 s(t) + n_1(t), \tag{80}$$

where α_1 and n_1 denote the atmospheric fading and background noise for the source-to-relay ($S \to R$) channel. The relay transmits the photons to the destination with an average of m_2. The photon count due to background radiation is modeled by a negative binomial distribution (also known as Bose-Einstein) with an average of m_R [50,51,53]. The averages m_1, m_2 and m_R are related to the physical characteristics of the transmitter and the channel such as wavelength, transmit power, modulation rate, and the atmospheric conditions. Their exact calculations can be found in [51]. The total photon rate at the destination is given by

$$r_D(t) = G\alpha_2\alpha_1 s(t) + G\alpha_2 n_1(t) + \alpha_2 n_{ASE}(t) + n_2(t), \tag{81}$$

where α_2 and n_2 denote the atmospheric fading and the background noise of the relay-to-destination ($R \to D$) channel and G is the gain of the all-optical AF relay.

Recall that a log-normal distribution for the statistics of the atmospheric turbulence is assumed, therefore we have $\alpha_i = \beta_i \exp(2\chi_i)$, i=1,2, where β_i is the loss factor and χ_i is Gaussian distributed with mean $\mu_{\chi_i} = -\sigma^2_{\chi_i}$. Note that the link loss

($\beta_i \propto d^2$) and the turbulence fading ($\sigma_{\chi i} \propto d^{11/12}$) also depend on the link length.

The ASE is modeled by an additive noise (similar to the background noise) with a count of $m_{ASE} = n_{sp}(G-1)$ and M degree-of-freedom [51]. The value of M depends on both spatial and temporal filtering at the relay terminal. Assuming only one spatial mode, we have $M = 2B_o/B_e$ where B_o and B_e denote the equivalent optical and electrical bandwidths of optical filters. The factor n_{sp} denotes the spontaneous emission factor of the amplifier and can be approximately taken equal to unity for most practical purposes.

5.2 Outage Performance Analysis

Recall that at a target transmission rate of R_0, the outage probability can be expressed as $P_{out} = \Pr(\gamma_T \leq \gamma_{th})$ where γ_{th} is the minimum acceptable end-to-end SNR above which the quality of service, i.e. the desired transmission rate, is satisfied. Therefore, in practice, it should be chosen based on the type of application or service, e.g. voice communication, real-time video streaming, gaming etc. In the following, we first obtain the end-to-end SNR, and then use it for the derivation of the outage probability.

5.2.1 End-to-end SNR

The photon count statistics (denoted by k) at the destination obeys Laguerre distribution[1] [54]. The probability of k counts is given by

$$\begin{aligned} p_{count}(k) =& Lag(k, a, b, M) \\ =& \frac{b^k}{(1+b)^{k+M}} \exp\left(-\frac{a}{1+b}\right) L_k^{M-1}\left(-\frac{a}{b(1+b)}\right), \end{aligned} \tag{82}$$

where a and b denote the average photon counts for, respectively, the desired signal and the total background noise. In (82), $L_k^M(x)$is the generalized Laguerre polynomial

[1]Note that the receiver analyses here is developed from photoelectron-count statistics which is entirely equivalent to the Poisson process approach when the product of the signal pulse duration and photodetector's electrical bandwidth is much more than unity.

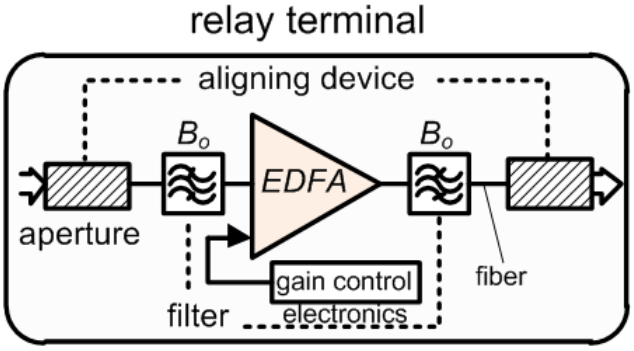

Figure 18: Mathematical model for all-optical AF relaying.

of degree k and defined as [55]

$$L_k^M(x) = \sum_{i=0}^{k} \frac{(-x)^i (k+M)!}{i!\,(k-i)!\,(M+i)!}.$$

In our case, we have $a = G\alpha_1\alpha_2 m_1$ and $b = m_R + G\alpha_2 m_R + \alpha_2 m_{ASE}$ based on (81). In practical situations, the average photon counts due to the background noise is much smaller than the average photons received at the relay (or destination), i.e., $\{m_R << \overline{\alpha_i} m_i, m_{ASE} | i = 1, 2\}$ where $\overline{\alpha_i} = E(\alpha_i)$ denotes the statistical average of the atmospheric fading. Hence, we have $b \cong \alpha_2 m_{ASE}$.

The end-to-end SNR of the system under consideration is given by $\gamma_T = a^2/\sigma_n^2$ where σ_n^2 is the variance of the photon counts at the receiver and can be expressed as $\sigma_n^2 = a + Mb(1+b) + 2ab$ for Laguerre distribution. In full-CSI relaying, the relay has the full knowledge of the instantaneous $S \to R$ channel condition and sets the amplifier gain to $G = m_2/(\alpha_1 m_1 + m_R) \cong m_2/\alpha_1 m_1$. In semi-blind relaying, the gain of the amplifier is fixed to $G = m_2/E(\alpha_1 m_1 + m_R) \cong m_2/m_1 E(\alpha_1)$. These choices of the amplifier gain aims to invert the fading effect of the source-to-relay channel while limiting the output power of the relay if the fading amplitude of the first hop, α_1 , is low [56]. Replacing G in γ_T, we have

$$\gamma_T^{-1} = \begin{cases} 2\hat{\gamma}_1^{-1} + M\hat{\gamma}_1^{-2} + \hat{\gamma}_2^{-1}, & \text{CSI-assisted} \\ M\hat{\gamma}_1^{-2} + \overline{\hat{\gamma}_1}\hat{\gamma}_1^{-1}\hat{\gamma}_2^{-1} + 2\hat{\gamma}_1^{-1}, & \text{semi-blind} \end{cases} \tag{83}$$

where $\hat{\gamma}_i = m_i\alpha_i, i = 1, 2$ denotes the conditional SNR of link i.

5.2.2 Outage Probability

The instantaneous SNR for the ith link is given by $\hat{\gamma}_i = \gamma_{avg,i} \exp(2\chi_i)$ where $\gamma_{avg,i} = m_i\beta_i$. It obeys a log-normal distribution with pdf which is denoted by $p(\hat{\gamma}_i)$. The outage probability can be then expressed as

$$P_{out} = \Pr(\gamma_T \leq \gamma_{th}) = \int_0^\infty \Pr(\gamma_T \leq \gamma_{th}|\hat{\gamma}_1) p(\hat{\gamma}_1) d\hat{\gamma}_1. \tag{84}$$

For full-CSI relaying, this yields

$$\begin{aligned} P_{out} &= \int_0^{\gamma^*} \Pr\left(\hat{\gamma}_2 \geq \left(\gamma_{th}^{-1} - 2\hat{\gamma}_1^{-1} - M\hat{\gamma}_1^{-2}\right)^{-1} \middle| \hat{\gamma}_1\right) p(\hat{\gamma}_1) d\hat{\gamma}_1 \\ &+ \int_{\gamma^*}^\infty \Pr\left(\hat{\gamma}_2 \leq \left(\gamma_{th}^{-1} - 2\hat{\gamma}_1^{-1} - M\hat{\gamma}_1^{-2}\right)^{-1} \middle| \hat{\gamma}_1\right) p(\hat{\gamma}_1) d\hat{\gamma}_1 \\ &= 1 - Q\left(\frac{0.5\ln(\gamma^*/\gamma_{avg,1}) - \mu_1}{\sigma_1}\right) \\ &+ \int_{\gamma^*}^\infty \left(1 - Q\left(\frac{0.5\ln(\gamma_{TH,CSI}/\gamma_{avg,2}) - \mu_2}{\sigma_2}\right)\right) p(\hat{\gamma}_1) d\hat{\gamma}_1, \end{aligned} \tag{85}$$

where $\gamma_{TH-CSI}^{-1} = \gamma_{th}^{-1} - 2\hat{\gamma}_1^{-1} - M\hat{\gamma}_1^{-2}$. In (85), the lower limit on the integral γ^* is the first positive (non-zero) solution of $\gamma_{th}^{-1} - 2\hat{\gamma}_1^{-1} - M\hat{\gamma}_1^{-2} = 0$ for γ_1 and given by $\gamma^* = M/\left(\sqrt{1 + M\gamma_{th}^{-1}} - 1\right)$.

For semi-blind relaying, we have

$$\begin{aligned} P_{out} &= \int_0^{\gamma^*} \Pr\left(\hat{\gamma}_2 \geq \left(\frac{\overline{\hat{\gamma}_1}\hat{\gamma}_1^{-1}}{\gamma_{th}^{-1} - 2\hat{\gamma}_1^{-1} - M\hat{\gamma}_1^{-2}}\right) \middle| \hat{\gamma}_1\right) p(\hat{\gamma}_1) d\hat{\gamma}_1 \\ &+ \int_{\gamma^*}^\infty \Pr\left(\hat{\gamma}_2 \leq \left(\frac{\overline{\hat{\gamma}_1}\hat{\gamma}_1^{-1}}{\gamma_{th}^{-1} - 2\hat{\gamma}_1^{-1} - M\hat{\gamma}_1^{-2}}\right) \middle| \hat{\gamma}_1\right) p(\hat{\gamma}_1) d\hat{\gamma}_1 \\ &= 1 - Q\left(\frac{0.5\ln(\gamma^*/\gamma_{avg,1}) - \mu_1}{\sigma_1}\right) \\ &+ \int_{\gamma^*}^\infty \left(1 - Q\left(\frac{0.5\ln(\gamma_{TH,SBR}/\gamma_{avg,2}) - \mu_2}{\sigma_2}\right)\right) p(\hat{\gamma}_1) d\hat{\gamma}_1, \end{aligned} \tag{86}$$

where γ_{TH-SBR}^{-1} is given by

$$\gamma_{TH-SBR}^{-1} = \frac{\gamma_{th}^{-1} - 2\hat{\gamma}_1^{-1} - M\hat{\gamma}_1^{-2}}{\overline{\hat{\gamma}_1}\hat{\gamma}_1^{-1}}. \tag{87}$$

5.3 Numerical Results

In this section, we present outage performance results. We assume that the relay is placed at equal distance from both source and destination, and the links are balanced (i.e., $\overline{\hat{\gamma}_1} = \overline{\hat{\gamma}_2}$). We consider an FSO system with the optical wavelength of 1550 nm operating in clear weather conditions with a visibility of 10 km. This leads to an attenuation factor of 0.1 per km. We assume a refractive index structure constant of $10^{-14}\text{m}^{2/3}$ for the overall channel (i.e., direct link between the source and destination) and fading variance $\sigma_\chi^2 = 0.3$. In our simulations, the SNR threshold is set as $\gamma_{th} = 15$ dB.

Fig. 19 illustrates the outage probability given by (85) and (86) for full-CSI and semi-blind all-optical AF relaying. As a benchmark, the performance of direct transmission is also provided. We also illustrate the performance for different values of DoF, i.e., $M = 1, 10, 100$ and 1000. Note that $M = 1$ is the ideal case where the effect of the DoF is not taken into account, while practical values of M range from 100 to 1000 [51]. For the ideal case (i.e., $M = 1$), at a target outage probability of 10^{-6}, relay-assisted transmission with full-CSI relay results in a performance gain of 14.7 dB in comparison to the direct transmission. This improvement comes from the fact that fading variance is distance-dependent in FSO channel and relay-assisted transmission takes advantage of the resulting shorter hops. The improvement reduces to 14.4 dB, 13.2 dB and 10.3 dB for $M = 10, 100, 1000$ respectively. Noting that practical values of M are in the range of 100 to 1000, a significant performance gain over direct transmission is still maintained. We further observe that for small values of M, systems with full-CSI relay outperform those with semi-blind relay. Specifically, for $M = 1$ (i.e., ideal case), the performance gap at $P_{out} = 10^{-6}$ is 3.4 dB. For more

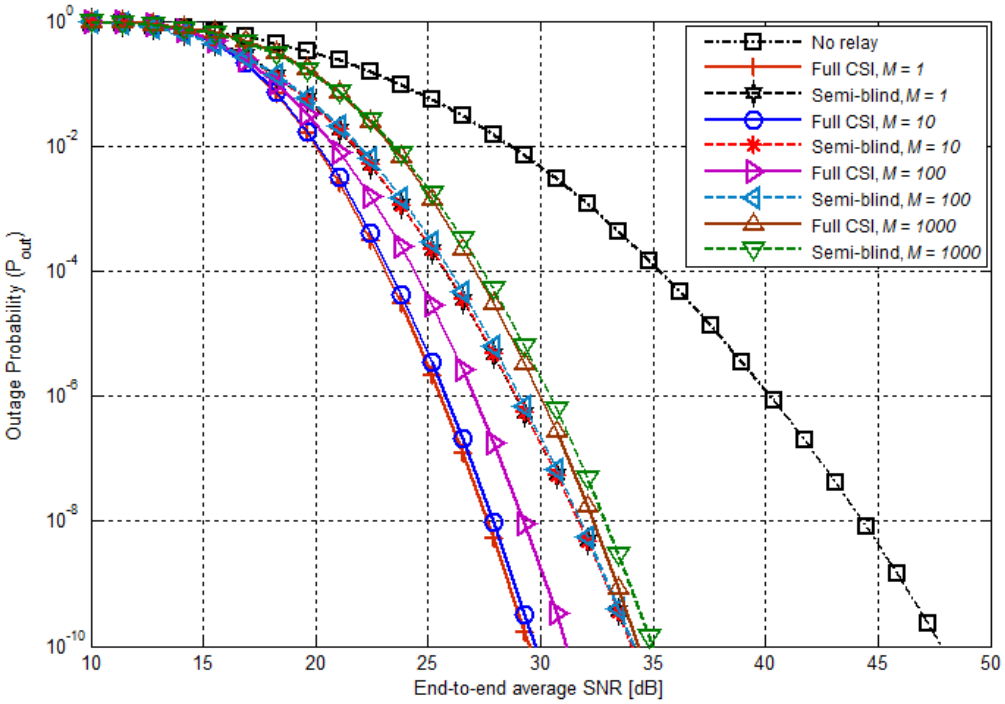

Figure 19: Outage probability of all-optical AF relaying.

practical values, this gap decreases and semi-blind relaying yields nearly the same performance as its full-CSI counterpart. For example, for $M = 1000$, the performance difference between semi-blind and full-CSI is merely 0.4 dB.

In Fig. 20, we present a comparison between all-optical AF relaying with $M = 1000$ and conventional AF relaying with OE/EO conversions. The outage probability of conventional AF relaying system can be obtained by applying the main results of [57–59] to lognormal atmospheric channels and is omitted here due to space constraints. Under the assumption of CSI-assisted relay, conventional relaying outperforms the all-optical counterpart. For semi-blind relay deployment, the performance of all-optical relaying is slightly worse than the conventional counterpart for low to medium SNR region and becomes nearly identical for high SNRs. It should be emphasized here that these results have been obtained for a relatively large value of DoF (i.e., $M = 1000$). The performance of all-optical relaying can be further improved by decreasing the value of M which is possible, in practice, by a better filter design. Our

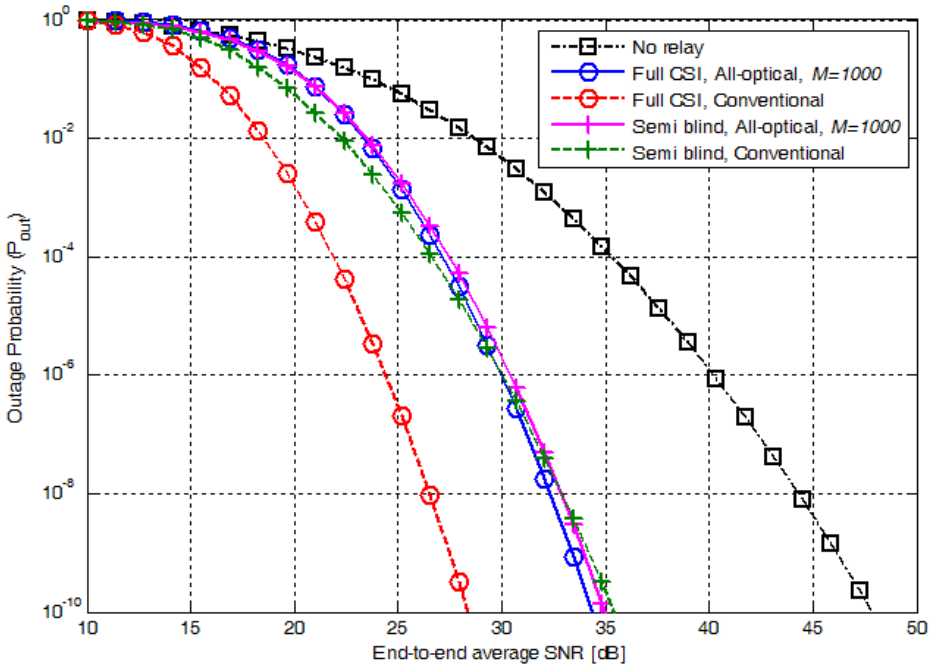

Figure 20: Outage probability for CSI-assisted and semi-blind relaying with optical and electrical amplification.

comparison demonstrates that semi-blind all-optical relaying presents a favourable trade-off between complexity and performance, and can be used as a low-complexity solution.

CHAPTER VI

CONCLUSIONS

Despite the major advantages of FSO technology and variety of its application areas, its widespread use has been hampered by its rather disappointing link reliability particularly in long ranges due to atmospheric turbulence-induced fading. Relay-assisted systems have been recently introduced in the literature as an effective method to extend coverage and mitigate the effects of fading in FSO links. This thesis has addressed several issues in the performance analysis and optimization of relay-assisted FSO communication

In Chapter 3, we have considered relay-assisted FSO links with DF relays and investigated the optimal relay placement problem for serial and parallel relaying along with a diversity gain analysis over log-normal turbulence channels. For serial relaying, we have demonstrated that the outage probability is minimized when the consecutive nodes are placed equidistant along the path from the source to the destination. For parallel relaying, we have found out that all of the relays should be located at the same place (along the direct link between the source and the destination) closer to the source and the exact location of this place depends on the system and channel parameters. As for diversity gain analysis, since the conventional definition of diversity order yields infinity and does not provide a meaningful measure over log-normal turbulence fading channels, we have adopted so-called relative diversity order (RDO) and quantified it in terms of the number of relays and channel parameters. Through an asymptotical analysis, we have demonstrated that diversity gains of $(N+1)^{11/6}$ and $2^{11/6}N$ are achievable (where N denotes the total number of relays) respectively for serial and parallel relaying.

In Chapter 4, we have investigated the combined use of serial (multi-hop) and parallel relaying for FSO mesh networks. In our set-up, the source node communicates with a destination node via the total of Nrelays. The nearby relays are grouped together resulting in a number of K groups. Under the assumption of DF relaying, we have derived outage probability expressions for the multi-hop parallel relaying scheme and quantified the diversity gain order. Our analysis yields that a diversity order of $(K+1)^{11/6}(N/K)$ is achievable for the multi-hop parallel relaying scheme under consideration.

In Chapter 5, we have focused our attention on all-optical relaying. Unlike the earlier relaying schemes, the signals are processed in optical domain and therefore avoid the requirement of OE and EO conversions. We have considered a dual-hop IM/DD FSO system with all-optical AF relaying. Based on photon counting approach, we have derived outage performance expressions over log-normal atmospheric fading channels for full-CSI and semi-blind relays. Our results have demonstrated significant performance gains over direct transmission even for high DoF values. We have also observed that, for the practical range of DoF values, semi-blind relaying provides a comparable performance to its full-CSI counterpart. Further comparisons between conventional and all-optical relaying demonstrate that the latter presents a favorable trade-off between complexity and performance and can be used as a low-complexity solution.

APPENDIX A

PROOFS OF THEOREMS

A.1 Proof of Theorem I

"*In serial relaying, optimum place for each relay is on the direct path from the source to the destination.*"

Proof by contradiction: Seeking a contradiction, assume that in the optimum configuration there exists at least one relay which is not on the path along the source to the destination. Let the i^{th} relay be that relay. Further let d'_i and d'_{i+1} denote the projections of d_i and d_{i+1} on the direct path. Therefore, we have

$$h\left(d_1,\ldots,d_i,d_{i+1},\ldots,d_{K+1}\right) \geq h\left(d_1,\ldots,d'_i,d'_{i+1},\ldots,d_{K+1}\right), \tag{88}$$

where $h\left(.\right)$ has been earlier defined in (11). Using (11) in (88), we obtain

$$\left(\Phi\left(f\left(d_i\right)\right)\Phi\left(f\left(d_{i+1}\right)\right)-\Phi\left(f\left(d'_i\right)\right)\Phi\left(f\left(d'_{i+1}\right)\right)\right)\times\prod_{\substack{\mathrm{j}=1\\ j\neq i,i+1}}^{K+1}\Phi\left(f\left(d_j\right)\right)\geq 0. \tag{89}$$

Note that $d'_i \leq d_i$, $d'_{i+1} \leq d_{i+1}$ and $f\left(d\right)$ is a monotonically decreasing function. Further considering the properties of Q function, it is obvious that$\Phi\left(f\left(d_i\right)\right)\Phi\left(f\left(d_{i+1}\right)\right) \leq \Phi\left(f\left(d'_i\right)\right)\Phi\left(f\left(d'_{i+1}\right)\right)$. Thus, (89) must be negative. This contradicts our original claim that in optimum configuration there is at least one relay not located in the direct line and concludes the proof.

A.2 Proof of Theorem II

"*In parallel relaying, optimal relays are located along the direct path from the source to the destination.*"

Proof by contradiction: The proof proceeds in a similar fashion to the proof of Theorem I. Again assume that in the optimal scheme there exists at least one relay not

located on the direct path. Let us assume that the i^{th} relay (with source-to-relay and relay-to-destination distances of $d_{S,i}$ and $d_{i,D}$) is not on the direct path. Let $d'_{S,i}$ and $d'_{i,D}$ denote the projections of $d_{S,i}$ and$d_{i,D}$ on the direct path. Therefore, we have

$$z(d_{S,1},\ldots,d_{S,i}\ldots,d_{i,D}\ldots,d_{K,D}) \leq z(d_{S,1},\ldots,d'_{S,i}\ldots,d'_{i,D}\ldots,d_{K,D}), \tag{90}$$

where $z\,(.)$ has been earlier defined by (18). Eq. (18) can be rewritten as

$$z(.) = \sum_{j=1}^{2^{K-1}} P_s(j)\left[Q\left(u(d_{S,i})\right)Q\left(v(\bar{d}_{W(i)})\right) + \left(1-Q\left(u(d_{S,i})\right)\right)Q\left(v(\bar{d}_{W(i)},d_{i,D})\right)\right]. \tag{91}$$

Inserting (91) in (90), we obtain

$$\left[Q_1-\hat{Q}_1\right]Q_M + (1-Q_1)\,\tilde{Q}_M - \left(1-\hat{Q}_1\right)\hat{Q}_M \leq 0, \tag{92}$$

where we have defined $Q_1 = Q\left(u(d_{S,i})\right)$, $Q_M = Q\left(v(\bar{d}_{W(i)})\right)$, $\hat{Q}_1 = Q\left(u(d'_{S,i})\right)$, $\tilde{Q}_M = Q\left(v(\bar{d}_{W(i)},d_{i,D})\right)$ and $\hat{Q}_M = Q\left(v(\bar{d}_{W(i)},d'_{i,D})\right)$. (92) can be rearranged as

$$\left[Q_1-\hat{Q}_1\right]Q_M + \left(1-\hat{Q}_1-\left(Q_1-\hat{Q}_1\right)\right)\times\left(\hat{Q}_M+\tilde{Q}_M-\hat{Q}_M\right) - \left(1-\hat{Q}_1\right)\hat{Q}_M \leq 0. \tag{93}$$

By expanding the second term, (93) yields

$$\left(Q_1-\hat{Q}_1\right)\left(Q_M-\hat{Q}_M\right) + (1-Q_1)\left(\tilde{Q}_M-\hat{Q}_M\right) \leq 0. \tag{94}$$

Noting $d'_{S,i} \leq d_{S,i}$, $d'_{i,D} \leq d_{i,D}$ along with the fact that $u\,(d)$ and $v\,(d)$ are monotonically decreasing functions, we find out that Q_1 and $\tilde{Q}_M$ are respectively larger than $\hat{Q}_1$ and $\hat{Q}_M$. Furthermore, it can be shown that $v(\bar{d}_{W(i)},d_{i,D}) \geq v(\bar{d}_{W(i)})$. Therefore, Q_M is larger than $\hat{Q}_M$. Thus, (94) turns out to be positive which contradicts our original hypothesis.

Bibliography

[1] H. Willebrand and B. Ghuman, *Free space optics: enabling optical connectivity in today's networks*. Sams Publishing, 2002.

[2] A. Majumdar and J. Ricklin, *Free-space laser communications: principles and advances*, vol. 2. Springer Verlag, 2008.

[3] L. Andrews, R. Phillips, and C. Hopen, *Laser beam scintillation with applications*, vol. 99. Society of Photo Optical, 2001.

[4] X. Zhu and J. Kahn, "Performance bounds for coded free-space optical communications through atmospheric turbulence channels," *IEEE Transactions on Communications*, vol. 51, no. 8, pp. 1233–1239, 2003.

[5] M. Uysal, J. Li, and M. Yu, "Error rate performance analysis of coded free-space optical links over gamma-gamma atmospheric turbulence channels," *IEEE Transactions on Wireless Communications*, vol. 5, no. 6, pp. 1229–1233, 2006.

[6] F. Xu, M. Khalighi, and S. Bourennane, "Coded PPM and multipulse PPM and iterative detection for free-space optical links," *Journal of Optical Communications and Networking*, vol. 1, no. 5, pp. 404–415, 2009.

[7] I. Djordjevic, "Coding for free space optical communications," in *21st Annual Meeting of the IEEE Lasers and Electro-Optics Society (LEOS 2008)*, pp. 884–885, IEEE, 2008.

[8] J. Anguita, M. Neifeld, B. Hildner, and B. Vasic, "Rateless coding on experimental temporally correlated fso channels," *Journal of Lightwave Technology*, vol. 28, no. 7, pp. 990–1002, 2010.

[9] X. Zhu and J. Kahn, "Markov chain model in maximum-likelihood sequence detection for free-space optical communication through atmospheric turbulence channels," *IEEE Transactions on Communications*, vol. 51, no. 3, pp. 509–516, 2003.

[10] X. Zhu, J. Kahn, and J. Wang, "Mitigation of turbulence-induced scintillation noise in free-space optical links using temporal-domain detection techniques," *IEEE Photonics Technology Letters*, vol. 15, no. 4, pp. 623–625, 2003.

[11] N. Chatzidiamantis, G. Karagiannidis, and M. Uysal, "Generalized maximum-likelihood sequence detection for photon-counting free space optical systems," *IEEE Transactions on Communications*, vol. 58, no. 12, pp. 3381–3385, 2010.

[12] A. Paulraj, R. Nabar, and D. Gore, *Introduction to space-time wireless communications*. Cambridge Univiversity Press, 2003.

[13] S. Haas and J. Shapiro, "Capacity of wireless optical communications," *IEEE Journal on Selected Areas in Communications*, vol. 21, no. 8, pp. 1346–1357, 2003.

[14] E. Lee and V. Chan, "Part 1: Optical communication over the clear turbulent atmospheric channel using diversity," *IEEE Journal on Selected Areas in Communications*, vol. 22, pp. 1896–1906, Nov. 2004.

[15] S. Wilson, M. Brandt-Pearce, Q. Cao, and M. Baedke, "Optical repetition MIMO transmission with multipulse PPM," *IEEE Journal on Selected Areas in Communications*, vol. 23, no. 9, pp. 1901–1910, 2005.

[16] S. Navidpour, M. Uysal, and M. Kavehrad, "BER performance of free-space optical transmission with spatial diversity," *IEEE Transactions on Wireless Communications*, vol. 6, no. 8, pp. 2813–2819, 2007.

[17] N. Cvijetic, S. Wilson, and M. Brandt-Pearce, "Receiver optimization in turbulent free-space optical MIMO channels with APDs and Q-ary PPM," *IEEE Photonics Technology Letters*, vol. 19, no. 2, pp. 103–105, 2007.

[18] I. Djordjevic, S. Denic, J. Anguita, B. Vasic, and M. Neifeld, "LDPC-coded MIMO optical communication over the atmospheric turbulence channel," *Journal of Lightwave Technology*, vol. 26, no. 5, pp. 478–487, 2008.

[19] N. Letzepis, I. Holland, and W. Cowley, "The gaussian free space optical mimo channel with q-ary pulse position modulation," *IEEE Transactions on Wireless Communications*, vol. 7, no. 5, pp. 1744–1753, 2008.

[20] M. Simon and V. Vilnrotter, "Alamouti-type space-time coding for free-space optical communication with direct detection," *IEEE Transactions on Wireless Communications*, vol. 4, no. 1, pp. 35–39, 2005.

[21] M. Safari and M. Uysal, "Do we really need OSTBCs for free-space optical communication with direct detection," *IEEE Transactions on Wireless Communications*, vol. 7, no. 11, pp. 4445–4448, 2008.

[22] E. Bayaki, R. Schober, and R. Mallik, "Performance analysis of MIMO free-space optical systems in gamma-gamma fading," *IEEE Transactions on Communications*, vol. 57, no. 11, pp. 3415–3424, 2009.

[23] M. Uysal, *Cooperative communications for improved wireless network transmission: framework for virtual antenna array applications.* Information Science Publishing, 2010.

[24] A. Acampora and S. Krishnamurthy, "A broadband wireless access network based on mesh-connected free-space optical links," *IEEE Personal Communications*, vol. 6, no. 5, pp. 62–65, 1999.

[25] J. Akella, M. Yuksel, and S. Kalyanaraman, "Error analysis of multi-hop free-space optical communication," *in Proc. IEEE International Conference on Communications (ICC)*, vol. 3, pp. 1777–1781, May 2005.

[26] T. Tsiftsis, H. Sandalidis, G. Karagiannidis, and N. Sagias, "Multihop free-space optical communications over strong turbulence channels," *in Proc. IEEE International Conference on Communications (ICC)*, vol. 6, pp. 2755–2759, Jun. 2006.

[27] G. Karagiannidis, T. Tsiftsis, and H. Sandalidis, "Outage probability of relayed free space optical communication systems," *Electronics Letters*, vol. 42, pp. 994–995, Aug. 2006.

[28] M. Safari and M. Uysal, "Relay-assisted free-space optical communication," *IEEE Transactions on Wireless Communications*, vol. 7, pp. 5441–5449, Dec. 2008.

[29] M. Karimi and M. Nasiri-Kenari, "BER analysis of cooperative systems in free-space optical networks," *IEEE/OSA Journal of Lightwave Technology*, vol. 27, pp. 5639–5647, Dec. 2009.

[30] M. Karimi and M. Nasiri-Kenari, "Outage analysis of relay-assisted free-space optical communications," *IET Communications*, vol. 4, no. 12, pp. 1423–1432, 2010.

[31] M. A. Kashani, M. Safari, and M. Uysal, "Optimal relay placement and diversity analysis of relay-assisted free-space optical communication systems," *under review in IEEE/OSA Journal of Optical Communications and Networking.*

[32] M. A. Kashani, M. M. Rad, and M. Uysal, "All-optical amplify-and-forward relaying system for atmospheric channels," *under review in IEEE Communications Letters.*

[33] M. A. Kashani and M. Uysal, "Outage performance and diversity gain analysis of free-space optical multi-hop parallel relaying," *under review in IEEE/OSA Journal of Optical Communications and Networking.*

[34] M. A. Kashani, M. Safari, and M. Uysal, "Optimal relay placement in cooperative free-space optical communication systems," in *IEEE WCNC 2012*, IEEE, April,2012.

[35] M. A. Kashani and M. Uysal, "Outage performance of FSO multi-hop parallel relaying," in *IEEE SIU 2012*, IEEE, April,2012.

[36] M. Karimi and M. Nasiri-Kenari, "Outage analysis of relay-assisted free-space optical communications," *IET Communications*, vol. 4, no. 12, pp. 1423–1432, 2010.

[37] C. Datsikas, K. Peppas, N. Sagias, and G. Tombras, "Serial free-space optical relaying communications over gamma-gamma atmospheric turbulence channels," *IEEE/OSA Journal of Optical Communications and Networking*, vol. 2, no. 8, pp. 576–586, 2010.

[38] N. Olsson, "Lightwave systems with optical amplifiers," *Journal of Lightwave Technology*, vol. 7, no. 7, pp. 1071–1082, 1989.

[39] G. Osche, *Optical detection theory for laser applications*, vol. 51. Wiley-Interscience, 2002.

[40] D. Tse and P. Viswanath, *Fundamentals of Wireless Communication*. Cambridge University Press, 2005.

[41] J. G. Proakis, *Digital Communications*. McGraw-Hill, 2001.

[42] D. Goldberg, *Genetic algorithms in search, optimization, and machine learning*. Addison-Wesley Professional, 1989.

[43] C. Lee, H. Kang, and T. Park, "Dynamic sectorization of microcells for balanced traffic in cdma: genetic algorithms approach," *IEEE Transactions on Vehicular Technology*, vol. 51, pp. 63–72, Jan. 2002.

[44] C. Ngo and V. Li, "Fixed channel assignment in cellular radio networks using a modified genetic algorithm," *IEEE Transactions on Vehicular Technology*, vol. 47, pp. 163–172, Feb. 1998.

[45] M. Safari and M. Uysal, "Cooperative diversity over log-normal fading channels: performance analysis and optimization," *IEEE Transactions on Wireless Communications*, vol. 7, no. 5, pp. 1963–1972, 2008.

[46] M. Grötschel, L. Lovász, and A. Schrijver, "The ellipsoid method and its consequences in combinatorial optimization," *Combinatorica*, vol. 1, no. 2, pp. 169–197, 1981.

[47] J. Laneman, D. Tse, and G. Wornell, "Cooperative diversity in wireless networks: Efficient protocols and outage behavior," *IEEE Transactions on Information Theory*, vol. 50, no. 12, pp. 3062–3080, 2004.

[48] S. Kazemlou, S. Hranilovic, and S. Kumar, "All-optical multihop free-space optical communication systems," *Journal of Lightwave Technology*, vol. 29, no. 18, pp. 2663–2669, 2011.

[49] E. Bayaki, D. Michalopoulos, and R. Schober, "Edfa-based all-optical relaying in free-space optical systems," in *IEEE Vehicular Technology Conference (VTC Spring)*, pp. 1–5, IEEE, 2011.

[50] E. Desurvire, *Erbium-Doped Fiber Amplifiers*. Wiley, 1994.

[51] M. Razavi and J. Shapiro, "Wireless optical communications via diversity reception and optical preamplification," *IEEE Transactions on Wireless Communications*, vol. 4, no. 3, pp. 975–983, 2005.

[52] S. Rosenberg and M. Teich, "Photocounting array receivers for optical communication through the lognormal atmospheric channel. 2: Optimum and suboptimum receiver performance for binary signaling," *Applied optics*, vol. 12, no. 11, pp. 2625–2635, 1973.

[53] H. Haus and J. Mullen, "Quantum noise in linear amplifiers," *Physical Review*, vol. 128, no. 5, p. 2407, 1962.

[54] J. Peina, "Superposition of coherent and incoherent fields," *Physics Letters A*, vol. 24, no. 6, pp. 333–334, 1967.

[55] Gradshteĭ, *Table of integrals, series, and products.*

[56] J. Laneman and G. Wornell, "Energy-efficient antenna sharing and relaying for wireless networks," in *IEEE Wireless Communications and Networking Conference (WCNC)*, vol. 1, pp. 7–12, IEEE, 2000.

[57] D. Da Costa and S. Aïssa, "End-to-end performance of dual-hop semi-blind relaying systems with partial relay selection," *IEEE Transactions on Wireless Communications*, vol. 8, no. 8, pp. 4306–4315, 2009.

[58] M. Hasna and M. Alouini, "A performance study of dual-hop transmissions with fixed gain relays," *IEEE Transactions on Wireless Communications*, vol. 3, no. 6, pp. 1963–1968, 2004.

[59] M. Hasna and M. Alouini, "End-to-end performance of transmission systems with relays over rayleigh-fading channels," *IEEE Transactions on Wireless Communications*, vol. 2, no. 6, pp. 1126–1131, 2003.

VITA

Mohammadreza A. Kashani was born in Tehran, Iran on September 17th, 1988. He received his B.Sc. from University of Tehran in Electrical and Computer Engineering in 2010. He is currently a graduate student and research assistant at Özyeğin University, Istanbul. He is working with Professor Murat Uysal. His current research interests include free-space optical communications, optical fiber communication, cooperative communications, and wireless communications. During his M.Sc. studies he has already published two conference papers along with another three journal papers under review on these topics.